Investigating the excitation mechanism of the C II λ6578 line in Planetary Nebulae

Master's Thesis
Master's degree in Astrophysics
Universidad de La Laguna
March 2023

Author: Elena Reyes Rodríguez
Supervisors: Dr. Jorge García Rojas
Dr. José Eduardo Méndez Delgado

Contents

RESUMEN

Comprender los mecanismos de excitación de las líneas débiles permitidas en nebulosas ionizadas es esencial para abordar adecuadamente el problema de la discrepancia de abundancias (DA). Este problema fundamental en nebulosas ionizadas consiste en que las abundancias de iones de elementos pesados obtenidas usando líneas de recombinación (LRs) débiles son sistemáticamente mayores a las estimadas usando líneas excitadas colisionalmente (LECs) del mismo ion. Si los niveles superiores que dan lugar a las líneas permitidas están poblados por bombeo de fotones del continuo (fluorescencia), la emisividad de la línea aumenta respecto al caso de recombinación pura y puede llevar a conclusiones erróneas.
El estudio de la contribución de la fluorescencia al flujo de la línea C II λ6578 en nebulosas planetarias es de especial interés debido a que esta línea se ha detectado en un gran número de objetos. Un trabajo reciente en el que se han utilizado datos de 76 nebulosas planetarias ha descubierto que, estadísticamente, la cinemática del gas desde el que se emite esta línea no se corresponde con lo que cabría esperar si el gas fuera químicamente homogéneo, sino que parece más coherente con la coexistencia de volúmenes de gas con distinta metalicidad. Las conclusiones de ese trabajo dependen de que C II λ6578 se origine mayormente por recombinación. Sin embargo, la influencia relativa de la fluorescencia del continuo en estos objetos puede ser importante e incluso dominar la emisión de C II λ6578.
En este trabajo investigaremos el mecanismo de excitación de esta línea utilizando una base de datos de espectros muy profundos de nebulosas ionizadas, observados por el grupo de investigación del IAC a lo largo de más de 20 años, usando principalmente telescopios de 8-10m. La metodología que se llevará a cabo consiste básicamente en el estudio del comportamiento de cocientes de intensidades de líneas de C II respecto al grado de ionización de las nebulosas.
Los resultados obtenidos confirman que las líneas de C II $\lambda\lambda$3918, 3920 están excitadas mayoritariamente por fluorescencia, las líneas de C II $\lambda\lambda$7231, 7236, 7237 pueden tener contribución tanto por fluorescencia como por recombinación; mientras que otras líneas provenientes de niveles de energía más altos (^{2}G ng and ^{2}F^o) nf, están excitadas por recombinación. Por otra parte, los resultados también reflejan que el mecanismo de excitación que domina en la transición que da lugar a la línea de C II λ6578 es la fluorescencia, siendo el canal de las líneas de C II λ3918, λ3920 el más importante, al menos para las regiones H II.

ABSTRACT

A proper understanding of the excitation mechanisms of faint permitted lines in ionized nebulae is essential to properly address the abundance discrepancy (AD) problem. This fundamental problem in ionized nebulae is that the abundances of heavy element ions obtained using faint recombination lines (RLs) are systematically higher than those estimated with collisional excited lines (CELs) of the same ion. If the upper levels that give rise to the permitted lines are populated by continuum photon pumping (fluorescence), the emissivity of the line is enhanced with respect to the case of pure recombination and can lead to erroneous conclusions.
The study of the fluorescence contribution to the C II λ6578 line flux in planetary nebulae is of particular interest because it has been detected in a large number of objects. A recent paper using data from 76 planetary nebulae has found that, statistically, the kinematics of the gas from which this line is emitted does not correspond to what would be expected if the gas were chemically homogeneous, but appears to be more consistent with the coexistence of gas volumes with different metallicity. The above conclusions depend on C II λ6578 originating mostly by recombination. However, the relative influence of continuum fluorescence in these objects may be important and even dominate the C II λ6578 emission.
In this project we will investigate the excitation mechanism of this line using a database of deep spectra of ionized nebulae, observed by the IAC research group over more than 20 years, by using mainly 8-10m type telescopes. The methodology to be applied would be basically on studying the behavior of C II line intensity ratios with respect to the degree of ionization of the nebulae.
The results obtained confirm that the C II $\lambda\lambda$3918, 3920 lines are mostly excited by fluorescence, C II $\lambda\lambda$7231, 7236, 7237 lines would have contributions from both starlight resonance fluorescence and recombination; while other lines coming from higher energy levels (^{2}G ng and ^{2}F^o) nf are excited by recombination. On the other hand, the obtained results clearly reflect that the excitation mechanism giving rise to the C II λ6578 line that dominates is fluorescence, being the channel of the C II λ3918, λ3920 lines more important, at least for the H II regions.

1 INTRODUCTION

1.1 Photoionized gaseous nebulae

Gaseous nebulae are bright and extended objects, reaching sizes from 1 light year (the typical size of a planetary nebula) up to hundreds of parsec for the largest H II regions (Aller 1984). Those with the highest surface brightness, as the Orion Nebula (Figure 1), can be observed even through small aperture telescopes. Although the surface brightness is not dependent on the distance, the more distant nebulae have greater interstellar extinctions. This is why the nearest nebulae tend to be the most-studied objects (Osterbrock & Ferland 2006).

Figure 1. From left to right: the planetary nebula NGC 2440, the very bright 30 Dor H II region in the Large Magellanic Cloud and the closest star forming region to our solar system, the Orion Nebula. Credits: Hubble Space Telescope images

Ionized gaseous nebulae are excited by ionizing radiation emitted by hot stars, or by non-thermal sources as is the case of supernova remnants (Aller 1984). In the case of the photoionized regions, the ultraviolet radiation from the ionizing stars is the source of energy that enables emission nebulae to radiate (Osterbrock & Ferland 2006). Among this group, there are H II regions and planetary nebulae (PNe). The first ones are regions of gas surrounding massive newly formed stars. The second ones are regions created with the ejection of the outer layers of gas in the last stages of low mass stars ($<$8 $M_\odot$).

The chemical composition of the gas in H II regions gives information about the current chemical composition of the Interstellar Medium (ISM) because they are very young objects and the stars inside them have not had time to contaminate the ISM with the products of their nuclear reactions. In contrast, PNe give information about the chemical composition when their progenitor star was formed (using elements that are not altered during the lifetime of the star, like O, Ne, Ar, S, etc.). However, other elements like He, C and N can be significantly modified during the lifetime of the star, providing information on the nucleosynthesis processes activated in the progenitor star.

The main physical idea that gives rise to the emission lines observed in nebular spectra is described below:

A hot star ($T_{\rm eff}$$>$30,000 K) emits a considerable amount of photons in the ultraviolet (UV) range. A H atom, the most abundant element in the Universe, contained in the surrounding gas of such star will take a few hours before interacting with an UV photon with an energy capable of taking out the electron ($h\nu$ $\geq$13.6 eV) (Ferland et al. 2016). This free electron will have a velocity fixed by the difference between the energy of the ionizing photon and the ionization potential of the hydrogen. Few seconds later, it will have an elastic collision with another free electron, "sharing" its kinectic energy. This is the mechanism of thermalization of the gas (Osterbrock & Ferland 2006). Once the Maxwellian distribution of velocities is reached, it can be parameterized by $T_{\rm e}$, the electron temperature. The higher the global velocity of the free electrons, the higher $T_{\rm e}$.

When the free electrons collide with some heavy ions, for example O^{2+} or O^{+}, they can excite them, because the global energy of the free electrons is proportional to $kT_{\rm e}$ (where k is Boltzmann's constant), while the energy levels of those ions are also proportional to the same quantity. Once excited, the ions decay to the ground level through forbidden transitions, since in the low density conditions of the nebulae, radiative transitions dominate the collisional de-excitations (Osterbrock & Ferland 2006), giving rise to CELs.

After a time of being released (on the order of years) (Ferland et al. 2016), a free electron can interact with a proton and recombine. This will form a H^0 atom. But recombination can occur in the excited levels of the atom, which decay to the fundamental level emitting H I RLs, such as Hα or Hβ. This phenomenon can occur with other ions too, including heavy elements. Once this cycle is finished, it starts again with a new photoionization, a few hours after recombination (Ferland et al. 2016).

In addition to the ionizing photons, the stellar sources emit a continuum of radiation with photons unable to ionize some elements, but excite them to higher levels. These excitations occur mostly between levels with the same spin multiplicity. This phenomenon is known as continuum pumping and is a fairly common type of fluorescence in ionized nebulae, being present in different ions such as [Ni II], [Fe II], [N I] or C II (Grandi 1975a, Grandi 1975b, Grandi 1976, Lucy 1995, Rodríguez 1999, Ferland et al. 2012). This type of excitation competes with pure recombinations or collisional excitations, being complex to model. Therefore, transitions affected by fluorescent excitations are often avoided in the study of the physical conditions and chemical abundances.

These basic principles are valid both for H II regions and PNe. The main difference is that PNe have hotter ionizing stars, which means that the proportion of very energetic photons is higher. This is often called a harder stellar source. The ionized gas in H II regions has, on average, electron densities of around 100 cm^{-3}, but in the brightest areas the density can reach values of 10^3–10^4 cm^{-3}, or even values $\sim$$10^5$–$10^6$ cm^{-3} as observed in some protoplanetary discs of the Orion nebula (Mesa-Delgado et al. 2012). In the case of PNe, it is common to find very high densities ($\sim 10^4$ cm^{-3}).

1.2 H II regions

Many important topics in astrophysics, such as the evolution of chemical elements and the star formation history of galaxies, involve the physics of ionized gas and the interpretation of their emission-line spectra. H II regions allow us to probe the evolution of the elements and star-formation history up to the outskirts of our own Galaxy, and in distant galaxies (Osterbrock & Ferland 2006). The reasons are that such nebulae are associated with recent outbursts of star formation and have an emission spectrum that can be observed at large distances in the Universe.

These regions are mainly located in the arms of spiral galaxies and in irregular galaxies. They show different sizes and shapes as their geometry is related to their progenitor molecular clouds. H II regions range from ultra-compact to giant ones, which can reach sizes of hundreds of parsec. Its size is characterized by the Strömgren radius (Equation 1), and depends mainly on the availability of ionizing photons from the ionizing sources and on the density of the region. The aforementioned equation considers a nebula composed only of hydrogen. It should be emphasized that the Strömgren sphere (the sphere with radius equal to the Strömgren radius) is an idealized model of an ionized nebula, which is useful for understanding the gas stratification to a first approximation.

$$r_1 = \sqrt[3]{\frac{3Q(\mathrm{H}^0)}{4\pi n^2_{\mathrm{H}^0}\alpha_{\mathrm{B}}(\mathrm{H}^0, T)}}. \tag{1}$$

$Q(\mathrm{H}^0)$ is the number of ionizing photons per unit of time, n_{H^0} is the particle density of H^0 [cm^{-3}] and $\alpha_{\mathrm{B}}(\mathrm{H}^0, T)$ is the recombination coefficient.

H II regions can reach electron temperatures of around $\sim$10,000 K and they have typical densities of 10^2-10^3 cm^{-3}, implying that the total masses range between 10^2-10^4 solar masses. The largest H II regions can contain hundreds of young stars. Therefore, the gas is being ionized by ultraviolet (UV) radiation from one, several or a cluster of massive stars of early O and B spectral types with effective temperatures around $3{\times}10^4 - 5 \times 10^4$ K. At these temperatures, the nebula is composed of fully ionized hydrogen, once-ionized helium and other elements in different ionization states.

1.3 Planetary Nebulae

PNe are a key end-point in the evolution of low-to-intermediate mass stars ranging from $\sim$1 to 8 $M_\odot$ (Frew et al. 2013) and present a relatively large age and metallicity spread (Maciel et al. 2009).

PNe allow us to look into the outer remaining envelopes of dying stars (Osterbrock & Ferland 2006). A PN is an expanding ionized shell of gas that was ejected during the asymptotic giant branch (AGB) phase of the stellar progenitor. The nebula is ionized by a hot central star (Frankowski & Soker 2009), typically with an effective temperature, $T_{\rm eff}$, between 30,000 K to 150,000 K, even hotter than galactic OB stars, and often less luminous ($M_V = -3$ to $+5$) (Osterbrock & Ferland 2006).

The PN shell is quite dense (electron densities between 10^3 to 10^5 cm^{-3}) compared to typical values for H II regions, while the region between the central star and the shell has a very low density (Frankowski & Soker 2009). In addition, the ionized shell shows a stratified structure, with the more ionized species being closer to the central star. The ionization structure also shows an expansion velocity gradient, with larger expansion velocities towards the external zones where the less ionized species are found (Ruiz-Escobedo & Peña 2022). The typical expansion velocity of the ionized shells in PNe are of the order of several times the velocity of sound ($\sim$25 km s^{-1}) (Osterbrock & Ferland 2006). Due to the progressive expansion, and the consequent decrease in density, the PNe progressively lose brightness until they are no longer detected. Such gaseous nebulae have relatively short lifetimes, of the order of a few 10^4 years.

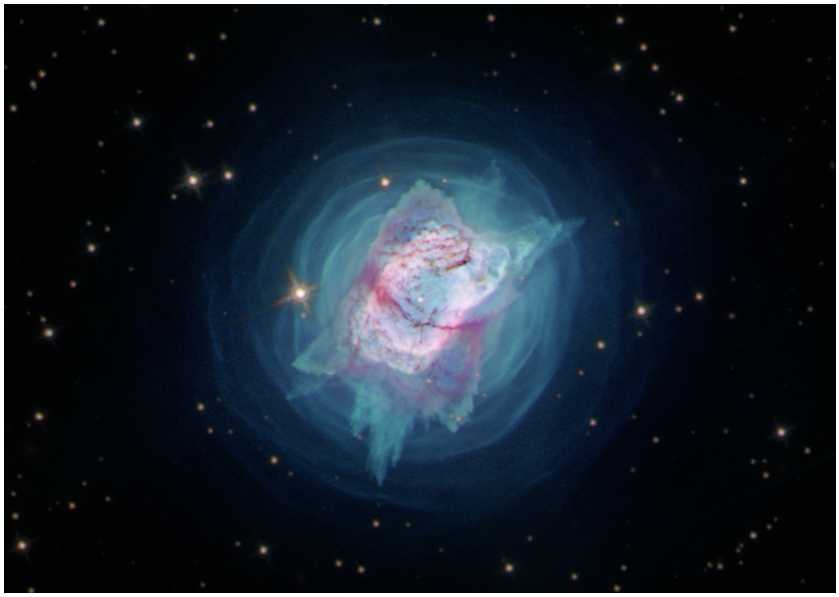

Figure 2. NGC 7027, a very young and compact PN. Credits: Hubble Space Telescope.

1.4 A more detailed view of the excitation mechanisms

In the following we are going to describe the three main mechanisms by which the spectral lines seen in nebular spectra can be generated: (i) collisional excitation, (ii) recombination and (iii) fluorescence.

(i) Collisional excitation

Collisional excitation is caused by the thermal electrons that are energized by photoionization. Collisions between free electrons and ions can excite bound electrons that occupy the lower energy levels of the heavy element ions, as they have levels of energies close to $kT_{\rm e}$[1]. Radiative decays of those excited levels have very low transition probabilities, between 10^{-4} and 1 s^{-1}. However, at the typical electron densities of the interstellar medium ($<10^4$ cm^{-3}) the collisional de-excitation is even less likely. Therefore, almost all collisional excitations are followed by a radiative decay: the resulting emission lines are known as collisionally excited lines (CELs).

For a given CEL, the emission rate resulting from the radiative transition between the upper level i and the lower level j can be calculated as (Osterbrock & Ferland 2006):

[1] k is the Boltzmann constant and $T_{\rm e}$ is the electron temperature of the gas.

$$j_\lambda = j_{ij} = \frac{h\nu_{ij}}{4\pi} n_i A_{ij} N(X^{+l}), \tag{2}$$

where $h\nu_{ij}$ is the energy difference between the levels involved in the transition, n_i is the relative population at the top level i of the +l times ionized element X, A_{ij} is the probability of radiative transition between these levels and $N(X^{+l})$ is the density of the ion responsible for the emission. As we can see, in order to determine the emissivity of a CEL, it is necessary to have information about the population of the starting level, and it is necessary to solve the statistical equilibrium equations, which is not a trivial task.

An important concept when studying environments where collisions may be relevant, is the critical density, $n_{i,c}$. This is the value at which collisional de-excitations are as likely as radiative de-excitations. For a given transition from level i it is defined as (Osterbrock & Ferland 2006):

$$n_{i,c} = \frac{\sum_{j<i} A_{ij}}{\sum_{j\neq i} q_{ij}}, \tag{3}$$

where q_{ij} is the collisional de-excitation rate.

The value of the critical density determines the turning point between a low density regime and a high density regime and its value increases as the level increases, i.e., it will be higher for higher atomic levels. Thus, for densities above the critical density, collisional de-excitations can be important and should be considered.

CELs can be divided according to the type of electronic transition involved and its behavior with the electric dipole interaction selection rules: permitted, semi-forbidden (which are electric dipole (E1) transitions for which the selection rule that the spin does not change is violated) and forbidden lines (these violate the selection rules of an electric dipole interaction). For example, the C IV line in UV is a permitted CEL, lines from C III] λ1906+1909 are semi-forbidden CELs and [O III] λ4957, λ5007 are forbidden CELs, respectively. The latter two have transition probabilities of the order of 10^{-2} s^{-1}. While the permitted lines have transition probabilities of the order of 10^{8} s^{-1}.

As we pointed out before, the emissivity of a CEL is directly proportional to the probability of radiative transition between the levels involved in the transition; this probability is an exponential function of the electron temperature, T_e, making the chemical abundances computed from CELs quite T_e-dependent.

(ii) Recombination

Recombination is a process of electron capture. If electrons recombine to excited levels, then they progressively decay to less energetic levels through cascade radiative decays, and may even decay to the fundamental level. From this process, emission lines known as recombination lines (RLs) are generated, which are permitted lines, as they are transitions that fulfil the selection rules of a dipole-electric interaction. The intensity of such lines is proportional to the electron density, the density of the element that gives rise to them and to a power of temperature close to one (Osterbrock & Ferland 2006). This makes the RL intensity ratios proportional to the relative chemical abundances, being almost independent of the physical conditions of the gas. Therefore, the RLs of heavy elements, such as those of C II, allow us to calculate the chemical abundances of ionized nebulae with a precision that depends directly on the quality of the spectra. A big number of lines with a high signal to noise ratio will be detected in deep spectra with high resolution. However, as mentioned previously, the presence of fluorescent mechanism will invalidate the proportionality between the line intensity ratios and the chemical abundances. Therefore, it is important to correctly characterize the dominant excitation mechanisms in order not to lead to erroneous chemical abundances.

The emission rate of a RL that is generated between levels nL and n′L′ can be written as (Osterbrock & Ferland 2006):

$$j_\lambda = j_{nn'} = \frac{h\nu_{nn'}}{4\pi} N_i n_e \alpha^{eff}_{nn}, \tag{4}$$

where $h\nu_{nn'}$ is the energy difference between the levels involved in the transition and α^{eff}_{nn} is the effective recombination coefficient, which expresses the probability that an electron in level nL will cascade down to level n′L′, taking into account all possible paths. Here, n and n′ are the principal quantum numbers of the levels and L and L′ the total angular momentum.

The strongest RLs in ionized nebula spectra are the H I lines, which are emitted from the recombination of electrons with H^+ ions; He I lines, emitted in He^+ recombination cascade; and He II lines, from recombination cascade of He^{2+} (Osterbrock & Ferland 2006). It is also possible to detect RLs emitted by heavy element ions, for example C II λ4267, λ5342, λ6151, λ6462 and λ9903. These RLs are several orders of magnitude weaker than hydrogen RLs, about 4-orders of magnitude weaker than Hα, because the ions that produce them are much less abundant in H II regions and PNe. Another case is the [C I] $\lambda\lambda$ 9850+23 lines, which are excited by recombination but decay as a forbidden transition (Escalante 1989).

(iii) Fluorescence

Fluorescence is another important mechanism giving rise to permitted lines of heavy elements. This mechanism can be generated by photons from the stellar continuum or photons from previous recombinations. These processes achieve the population inversion and are called pumping mechanism. This maintains a higher population of atoms in the upper energy level relative to that in the lower level. In Figure 3 we show the Grotrian diagram showing the permitted electronic transitions between the energy levels of C II (adapted from (Moore & Merrill 1968)). Levels ^{2}S $4s$ and ^{2}D $3d$ are directly interconnected to the ground state ^{2}P^0 $2p$ which means that they can be potentially populated through UV continuum photon pumping emitted at ∼638 Å and ∼687 Å respectively.

Some lines excited by fluorescence are sensitive diagnostics of the details of the stellar energy distribution (SED), the expansion velocity gradient and the turbulence of an ionized region. The comparison of predicted and observed intensities of fluorescence lines can be used to estimate the accuracy of calculations of the transition probabilities involved in the pumping mechanism. Ionic abundances deduced from dipole-permitted lines assuming pure recombination rates without taking into account fluorescence excitation of the lines can be overestimated by factors of up to 10 for C II depending on the transition being considered, and a detailed stellar energy distribution (SED) and nebular photoionization model are needed to properly estimate ionic abundances from lines mostly excited by fluorescence (Escalante et al. 2012).

The interpretation and understanding of the fluorescence emission lines depends on several hard-to-know factors, making this a rather complex mechanism. So these lines are usually not used as chemical abundance diagnostics in ionized regions, but it is important to know which lines are affected by fluorescence in order to avoid inappropriate analyses, such as the case of C II λ6578.

Seaton (1968) and Grandi (1975, 1976) suggested that continuum fluorescence of starlight is a mechanism that efficiently excites several permitted lines in H II regions and PNe. Escalante et al. (2012) compared calculated intensities of lines of different ions (C II, N I, N II, O I and O II) with a published deep spectrum of the PN IC 418; these authors proposed that fluorescence also contributes to the excitation of most lines of the s, p and d states in C II and some p and d states of O II, while the rest of the O II states are mostly excited by recombination. In Esteban et al. (1998) there is an extensive discussion on which heavy element permitted lines can be affected by fluorescence in the Orion nebula.

It is important to differentiate between these three processes, because for more than 80 years, it has been known that the abundances (relative to hydrogen) obtained from optical RLs of heavy elements are systematically higher than those obtained from the more commonly used, and much more intense, CELs. This Abundance Discrepancy (AD) is usually characterized by the ratio between the ion abundances obtained from optical RLs and CELs for a given ion and has values between 2 and 4 in H II regions and in most PNe. The existence of this discrepancy is one of the major unsolved problems in nebular astrophysics and has important implications for studies of the chemical evolution of the universe (García-Rojas et al. 2019; García-Rojas 2020). Therefore, a proper understanding of the excitation mechanisms of faint permitted lines in ionized nebulae is essential to properly address the AD problem. Escalante et al. (2012) propose that part of the observed AD in low excitation (and low AD) PNe may be due to fluorescence effects. In this project, the observed/predicted ratios in their Table 5 (for C II) will be useful

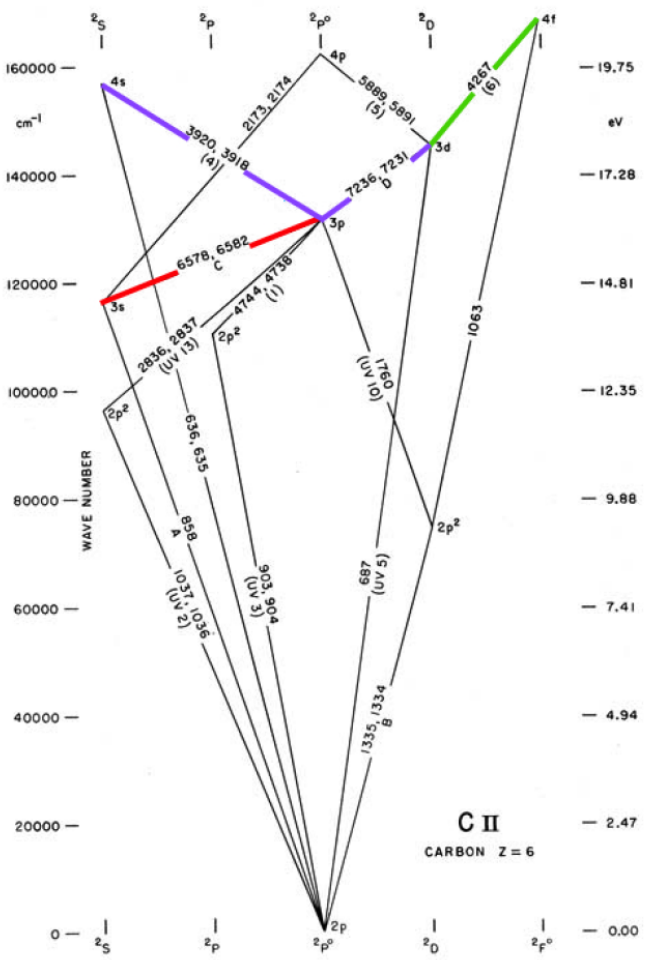

Figure 3. Grotrian diagram which shows the permitted electronic transitions between the energy levels of C II atom (Moore & Merrill 1968). In green we show the transition originating the C II λ4267 line which main excitation mechanism is recombination; in purple we show the transitions originating C II $\lambda\lambda$3918, 3920, 7231, 7236 and 7237 lines which are likely to be excited by photon pumping from the continuum. The analysed line in this project is shown in red. Its upper source level is interconnected with the emission of the C II $\lambda\lambda$3918, 3920, $\lambda\lambda$7231, 7236, 7237 lines, potentially excited by fluorescence. Values on the right represent the energy level separations with respect to the ground level.

for a comparison with our results.

The most important problem facing the study of the AD is the intrinsic faintness of heavy element optical RLs, generally three to four orders of magnitude fainter than the intensity of Hβ, which requires the use of high-resolution spectrographs and large-aperture telescopes. An additional problem is that recombination may not be the main excitation mechanism of these lines. The pioneering work of Grandi (1976) concluded that continuum fluorescence can excite the ^{2}S and ^{2}D terms of the C^+ ion so that some lines such as C II $\lambda\lambda$7231, 7236, 7237, coming from the upper ^{2}D level, may be strongly affected. In contrast, other optical lines like C II λ4267 can only come from C^{++} recombination. Looking at Table 5 in Escalante et al. (2012) it can be seen that lines with $I_{\rm rec}/I_{\rm calc}$ ratios close to 1 can be guaranteed to be pure RLs.

1.5 The importance of the C II λ6578 line

The case of the C II λ6578 line is particularly interesting as it has been detected in a large number of objects as it is very close to the Hα line. If this line were a pure recombination line, it could be considered instead of C II λ4267 for work related to the AD problem. However, as it is interconnected

with potentially fluorescence excited lines (C II $\lambda\lambda$3918, 3920, $\lambda\lambda$7231, 7236, 7237 lines), this effect is enhanced and can lead to erroneous conclusions.

In a recent work, Richer et al. (2017) presented spectroscopic observations of the C II λ6578 line for 83 lines of sight in 76 PNe at high spectral resolution, aimed to study the kinematics of this permitted line with respect to other permitted lines and CELs. The main result of this study was that the kinematics of the C II λ6578 line was not as expected if this line arises from the recombination of C^{++} ions or the fluorescence of C^{+} ions in ionization equilibrium in a chemically homogeneous nebula, but instead its kinematics was more consistent with the emission arising from a volume more internal than expected. Concerning the discrepancy between chemical abundances inferred from permitted and CELs in photoionized nebulae, their results imply that PNe commonly have multiple plasma components. To take into account the fluorescence contribution to the emissivity of the C II λ6578 line these authors computed a set of photoionization models with central stars (assumed to be a blackbody) spanning at least the temperature range 40,000 K–150,000 K, finding that fluorescence may contribute a significant fraction of the total emissivity in the C II λ6578 line, especially for models with low-temperature central stars (see their Figure 7, top row), but never dominating the total surface brightness in the line. However, as fluorescence is a complex phenomenon, a change in the initial assumptions, such as the atomic data, the channels of continuum pumping or the validity of the blackbody approximation, can change the conclusions substantially.

Although the excitation mechanisms of the C II permitted lines has been explored for some objects in the previous works of Grandi (1975a), Grandi (1975b), Grandi (1976), Escalante & Morisset (2005), Escalante et al. (2012), it has never been studied with a large, high-quality observational sample. In this project, we analyze the general excitation mechanisms of permitted C II lines by studying their behavior in a large set of high-quality photoionized region spectra. Through a simple and direct approach, by means of line intensities ratios, we intend to show the behavior of the excitation mechanisms of C II lines.

2 OBJECTIVES

The main goal of this project is to explore, for the first time, relations between C II permitted line intensities in a large set of PNe, together with Galactic and extragalactic H II regions, photoionized HH objects and ring nebulae, covering different degrees of ionization of the gas.

On the way to achieving the main objective, the following objectives have been fulfilled:

- Familiarization with the basic astrophysical concepts for the development of the project: spectral lines present in nebular spectra, atomic transitions, excitation mechanisms, abundance discrepancy problem, degree of ionization, etc.

- Design of a Python code to perform this direct analysis from ratios of line intensities of spectra included in DESIRED (see section 3.1).

- Verification that the lines coming from ^{2}D nd – ^{2}F^0 nf and ^{2}F^0 nf–^{2}G ng transitions (C II λ5341, λ6151, λ6462, λ9903 lines) are effectively RLs.

- The comparison of the observed flux ratios of the lines of C II λ3918, λ3920, λ4267, λ6578, λ7231, λ7236, λ7237 with the degree of ionization can give us direct information on the influence of fluorescence on the excitation of this lines in a direct and general way.

- Find which is the mechanism that dominates the transition that arises the C II λ6578 line through different intensity ratios (see section 3).

3 METHODOLOGY

The spectrum of a nebula shows the distribution of the flux of electromagnetic radiation as a function of wavelength. Depending on the spectral resolution (the dispersive capacity of a spectrograph), we will be able to observe to a greater or lesser extent the emission line profiles and to deblend or not close emission lines.

In a nebular spectrum a continuum is observed, whose formation is mainly given by: i) the free-bound continuum radiation at frequency ν resulting from recombinations of free e- with a certain velocity to level with $n \geq n_{\text{ground level}}$, and an ionization potential; (ii) the free-free (Bremsstrahlung) continuum emitted by free e- accelerated in Coulomb collisions[2] with cations of charge Z. In ionized nebulae most of these cations are H^+, He^+ and He^{++}; (iii) the two photons decay of the 2 ^{2}S level, which is populated by direct recombinations and by cascades following recombinations to higher levels (Osterbrock & Ferland 2006).

Besides the nebula's continuum emission, the spectra exhibit emission lines produced by collisional excitation, recombination or fluorescence, as described before. These lines allow us to infer certain physical parameters such as the electron temperature and density, and hence, derive the chemical composition of the nebula (Peimbert et al. 2017). A typical emission line spectrum (in this case from the PN NGC 3918) is shown in Figure 4.

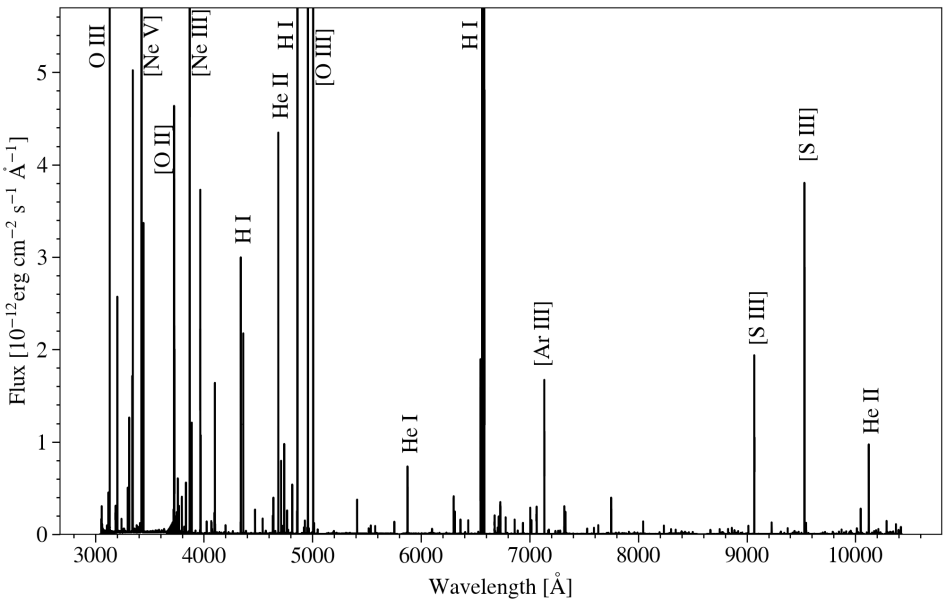

Figure 4. Spectrum of NGC 3918 taken with the Ultraviolet-Visual Echelle Spectrograph (UVES), attached to the 8.2 m Kueyen (UT2) Very Large Telescope (VLT) (García-Rojas et al. 2015). Some ions Y or [Y] have been highlighted in the graph, where [ ] means forbidden line. In this case, the ratio of the two [S III] lines is too low for what is expected by atomic physics, but this is due to the influence of telluric (sky) absorption bands affecting the λ9531 line.

3.1 DESIRED (DEep Spectra of Ionized REgions Database)

Since the beginning of this century, the IAC group has gathered many intermediate-to-high spectral resolution (R ~3,000 to ~33,000) long-slit or echelle spectra for many Galactic and extragalactic H II regions as well as Galactic PNe, photoionized HH objects and ring nebulae around very massive young stars. Most of the data have been obtained with large-aperture (8 – 10m) telescopes and the observations were designed to detect very faint emission lines. As a result of the remarkable depth of the observations, our collection of nebular spectra counts with tens or even hundreds of emission lines for each individual object, and contains good measurements of: (i) one or several faint electron temperature-sensitive auroral CELs, (ii) several density indicators based on the intensity ratios of CELs, (iii) ORLs of heavy-element

[2]Elastic collisions between charge particles, representing electron–electron, electron–ion, and ion–ion collisions

ions and (iv) sets of rare faint lines as those of [Fe II] and/or [Fe III] or fluorescence ones (Méndez-Delgado et al. submitted).

This database comprises a set of 190 spectra (72 of them correspond to extragalactic H II regions, 56 to Galactic H II regions, 34 to Galactic PNe, 21 to Galactic ring nebulae around massive stars, 6 to photoionized Herbig-Haro (HH) objects and 1 proplyd, the last two sets corresponding to objects immersed in the Orion Nebula). The database contains 29,381 emission line detections, associated with 2,486 transitions of 148 ionic species.

The different spectrographs used to obtain the spectra contained in this database were taken are shown in the Table 1. The telescope where the spectrographs are installed, the diameter of the primary mirror (M1) and its location have also been included.

Spectrograph	Telescope	M1 diameter [m]	Location
OSIRIS	GTC	10.4	La Palma, Spain
ISIS	WHT	4.2	La Palma, Spain
UVES	VLT	8.2	Paranal, Chile
FORS2	VLT	8.2	Paranal, Chile
MIKE	Clay Telescope	6.5	Las Campanas, Chile
MagE	Baade Telescope	6.5	Las Campanas, Chile
HIRES	KECK	10.0	Mauna Kea, Hawaii
Blanco echelle	CTIO Blanco	4.0	CTIO, Chile
Mayall echelle	KPNO Mayall Telescope	4.0	Arizona, USA

Table 1. Spectrographs with which the analyzed spectra were taken and the telescope where these are placed, the diameter of the primary mirror (M1) and its location.

More details can be found in Méndez-Delgado et al. (submitted), where details on the spectral resolution, wavelength coverage, and number of objects observed with each instrument are provided.

3.2 Analysis of the excitation mechanisms of C II lines

The spectral lines to be analyzed in this project are permitted C II lines, which are generally found in H II regions and PNe spectra. Lines in the region of the optical spectrum originating from C II transitions are permitted lines and we have analyzed a number of them in this project (Table 2 and Figure 5), including the line of main interest, C II λ6578.

Laboratory wavelength [Å]	Spc	Configuration	Term	Level energy [eV]
4267.001	C II	$2s^2.3d$-$2s^2.4f$	^2D-$^2F^o$	18.045808 - 20.950642
5342.500	C II	$2s^2.4f$-$2s^2.7g$	$^2F^o$-^2G	20.950695 - 23.270770
6151.530	C II	$2s^2.4d$-$2s^2.6f$	^2D-$^2F^o$	20.844773 - 22.859716
6461.950	C II	$2s^2.4f$-$2s^2.6g$	$^2F^o$-^2G	20.950695 - 22.868793
9903.890	C II	$2s^2.4f$-$2s^2.5g$	$^2F^o$-^2G	20.950695 - 22.202226
3918.978	C II	$2s^2.3p$-$2s^2.4s$	$^2P^o$-^2S	16.331742 - 19.494538
3920.693	C II	$2s^2.3p$-$2s^2.4s$	$^2P^o$-^2S	16.333124 - 19.494538
6578.048	C II	$2s^2.3s$-$2s^2.3p$	^2S-$^2P^o$	14.448827 - 16.333124
7231.340	C II	$2s^2.3p$-$2s^2.3d$	$^2P^o$-^2D	16.331742 - 18.045807
7236.420	C II	$2s^2.3p$-$2s^2.3d$	$^2P^o$-^2D	16.331742 - 18.045807
7237.170	C II	$2s^2.3p$-$2s^2.3d$	$^2P^o$-^2D	16.331742 - 18.045807

Table 2. Electronic configurations and energy levels of the different transitions that originate the C II lines of this project.

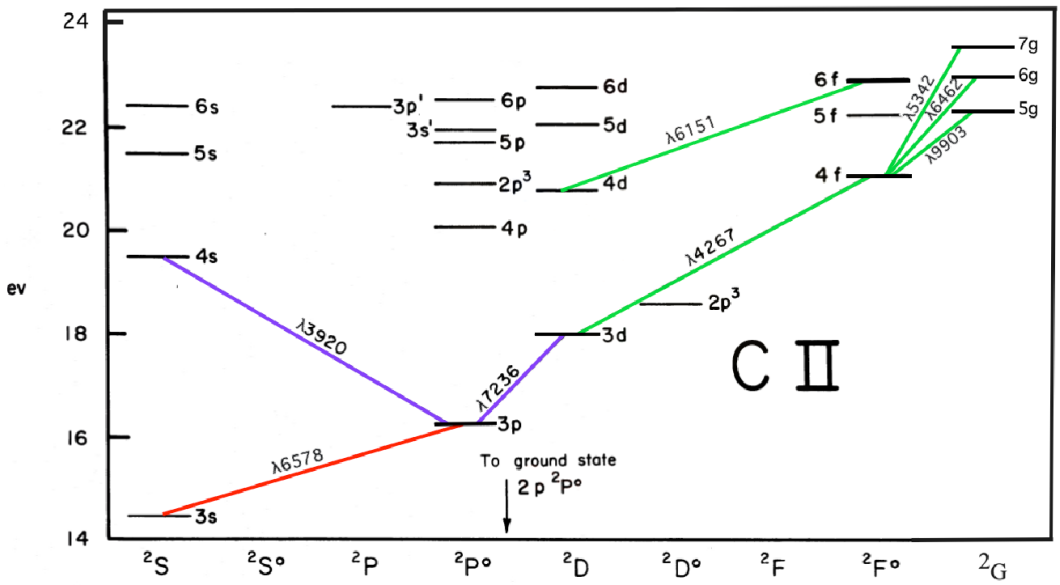

Figure 5. Grotrian diagram which shows the permitted electronic transitions between the energy levels of C II atom (Grandi 1976). In green we show the transitions originating the C II λ4267, λ5342, λ6151, λ6462, λ9903 lines which main excitation mechanism is recombination; in purple we show the transitions originating C II $\lambda\lambda$3920 and 7236[3] lines which are likely to be excited by photon pumping from the continuum. The analyzed line in this project is shown in red. Its upper source level is interconnected with the emission of the C II λ3920, λ7236 lines, potentially excited by fluorescence. Values on the left represent the energy level separations with respect to the ground level.

The ^{2}S and ^{2}D configurations are susceptible to excitation by UV photons from the ground level (see Figure 3). This means that the intensity of the lines originating from these levels is not entirely proportional to the recombinations of C^{++}, but also to the absorption of UV photons (continuum pumping) by C^+. Therefore, C II $\lambda\lambda$3918, 3920 lines can be generated by two main mechanisms: i) absorption of 638 Å photons by the C^+ and ii) direct recombinations of the C^{++} at the 4s level of the ^{2}S configuration. The first mechanism is fluorescence and the second recombination, the former generally being the one that dominates.

The case of the C II λ7231, λ7236, λ7237 lines is very similar, however, in this case there are three mechanisms at play: i) absorption of 687 Å photons by the C^+, ii) direct recombination of the C^{++} at the 3d level of the ^{2}D configuration and iii) cascade decays that give rise to the λ5889 and λ4267 lines. The first mechanism is fluorescence, whereas the other two are recombination (the λ4267 and λ5889 lines originate exclusively by recombination).

To populate the upper level of the C II λ6578 line, there are three main mechanisms at play: i) direct recombination, ii) cascade decays of the transitions giving rise to the C II λ7231, λ7236, λ7237 and iii) cascade decays of the transitions giving rise to the C II λ3918, λ3920 lines. The possible fluorescence effects, if any, to this line would come from the cascade decays of the transitions giving rise to the C II λ7231, λ7236, λ7237 and λ3918, λ3920 lines, because excitation of the 3p level of the ^{2}P^o configuration from the ground level is forbidden. So in the case the dominant excitation mechanism of these lines is fluorescence, the C II λ6578 line emissivity could be strongly affected.

We will now describe the methodology followed to carry on this project, in order to analyze the excitation mechanisms of the above transitions. The methodology is very direct: observed intensity ratios of C II permitted lines will be computed and represented *versus* the degree of ionization (in this case represented by a ratio of line intensities, not by an abundance ratio), measured as the following line

[3] C II λ3918 and λ3920 lines have the same electronic configuration, but the transition takes into account the fine structure: 3p $^2P^o_{1/2}$–4s $^2S_{1/2}$ and 3p $^2P^o_{3/2}$–4s $^2S_{1/2}$

C II λ7231, λ7236 and λ7237 lines have the same electronic configuration, but the transition takes into account the fine structure: 3p $^2P^o_{1/2}$–3d $^2D_{3/2}$, 3p $^2P^o_{3/2}$–3d $^2D_{5/2}$ and 3p $^2P^o_{3/2}$–3d $^2D_{3/2}$, respectively

ratio:

$$\frac{\mathrm{I}([\mathrm{OII}]\ 3727)}{\mathrm{I}([\mathrm{OIII}]\ 4959+5007)+\mathrm{I}([\mathrm{OII}]\ 3727)}, \tag{5}$$

where the intensities are found in files of the DESIRED database (Méndez-Delgado et al. submitted). Each of these files contains the theoretical wavelength, the ion, the observed wavelength of the spectral line, the observed and extinction corrected flux (which we called intensity) of the line as a function of the flux and the intensity of Hβ, respectively; the error in the intensity as a function of Hβ, and the full width half maximum (FWHM) and its error in units of km s^{-1}. It should be noted that the values of the ratio in Equation 5 increase from higher degree of ionization (lower ratio values) to lower degree of ionization (higher ratio values).

Relations between the intensities of permitted C II lines will be carried out systematically in a large set of photoionized regions from the DESIRED database, covering different degrees of ionization of the gas. The comparison of the observed flux ratios of the C II lines with the degree of ionization can give us direct information on the influence of fluorescence on the excitation of these lines.

As mentioned in the introduction, the intensity of a line is proportional to the number of particles of the emitting ion and an emissivity factor. This last value depends on the density and temperature of the gas in the case of non-fluorescent transitions, whereas other dependencies are expected in the presence of fluorescence, such as the optical depth or the effective temperature of the ionizing source. If the ratio of two C II permitted lines has a dependence on the degree of ionization, it is because the emission of one line is dependent on the C^{+} population, while the other on the C^{++} population. On the other hand, when both lines arises from recombinations, both are dependent on the C^{++} population. The dependence on the physical conditions in this case is also cancelled, showing a constant behaviour with the degree of ionization of the gas.

Firstly, the behavior according to the degree of ionization (Equation 5) of the pure RLs, such as C II λ4267, will be verified. Attending to the electronic configuration, we will look at C II $\lambda\lambda$ 4267, 5342, 6151, 6462, 9903 lines, which arise from very high levels that have no direct connection to the continuum pumping channels (see Figure 5). The line intensity ratios of these aforementioned lines are expected to be constant with respect to the degree of ionization. If these line intensity ratios are constant, the convergence will be tested with the predictions of the theoretical recombination coefficients of (Davey et al. 2000) (Péquignot et al. 1991) , considering a wide range of electron temperatures (4,000−15,000 K) and a typical electron density for PNe (10^3 cm^{-3}).

Secondly, to verify that the C II λ3918, λ3920 and C II λ7231, λ7236 and λ7237 lines are really fluorescent lines, the I(C II $\lambda 3918+20$)/I(C II λ4267) and I(C II $\lambda 72331+36+37$)/I(C II λ4267) ratios will be tested with respect to the degree of ionization.

Finally, we proceed to analyze the C II λ6578 line, which is line of greatest interest in our study (Figure 6 shows the spectrum region of NGC 3918 with C II λ6578 line). We will determine if this line is dominated by fluorescence or by recombinations. In addition, if it is fluorescent, we will determine the main channel of continuum pumping. All this systematic analysis uses PyNeb (Luridiana et al. 2015), a code created for the analysis of the line emission spectra. This code permits the efficient use of different atomic data bases.

As the atomic data is one of the input parameters of the photoionization models used in the analysis of PNe, we have to discuss some aspects of the main atomic data sets for C II found in the literature.

- Atomic data of Péquignot et al. (1991)
Péquignot et al. (1991)studied the total and effective radiative recombination coefficients for different ions, including other C ions. They consider a range of temperature of ∼5,000 K to ∼20,000 K and a low electron density. Here, the coefficients are presented in the form of simple fits, using four parameters: a, b, c and d.

- Atomic data of Davey et al. (2000)
Davey et al. (2000), considered the effective recombination coefficients for C II transitions between dou-

blet states in the temperature range 500-20,000 K and for an electron density of 10^4 cm^{-3}. They obtained the bound-bound and bound-free radiative data from a new calculation in which photoionization resonances are fully delineated, thus accurately incorporating both radiative and dielectronic recombination effects. In addition, they include the effects of electron collisions in the excited states.

Davey et al. (2000), compared their results with those of Péquignot et al. (1991), showing good agreement in most of the cases, except for the C II λ1335 line interconnected with the transition the $2s2p^2$ ^{2}D - $2s^22p$ ^{2}P^o, which have a relative difference of $\sim$92%. The difference arises from the dielectronic recombination that was not included in the calculations of Péquignot et al. (1991).

In both studies, the authors considered two different cases according to the treatment of the Lyman continuum emitted by the ionizing star (Aller et al. 1939): (i) case A and (ii) case B. Table 3 shows the case considered for each line used in this project.

(i) Case A: it is assumed that the nebula is optically thin to Lyman continuum (Péquignot et al. 1991). It is assumed that an electron enters quantum level n of an atom either by capture from the free state or by cascade from a higher discrete level. The radiation field of the star is neglected and there is not reabsorption of Lyman line radiation (Baker & Menzel 1938), and hence all the Lyman-line radiation can escape from the nebula.

(ii) Case B: the nebula is optically thick to Lyman continuum. The nebular radiation field must be taken into account by assuming that absorption from fundamental level to upper levels are balanced by the inverse spontaneous transitions, i.e, the radiation field is neglected (Baker & Menzel 1938). In this case, none of the Lyman-line radiation escapes, except Lyman α (Aller et al. 1939).

	Case A	Case B
D00	C II λ3920, C II λ4267, C II λ5342, C II λ6151, C II λ6462, C II λ6580, C II λ7235, C II λ9903	C II λ3920, C II λ4267, C II λ6151, C II λ7235, C II λ9903
P91	C II λ4267, C II λ6580, C II λ7231, C II λ9903	C II λ6580, C II λ7231

Table 3. C II lines associated to the atomic data included in PyNeb (Luridiana et al. 2015), which incorporates emissivity tables of RLs for a few atoms take into account the atomic data of Davey et al. (2000) (D00) and Péquignot et al. (1991) (P91).

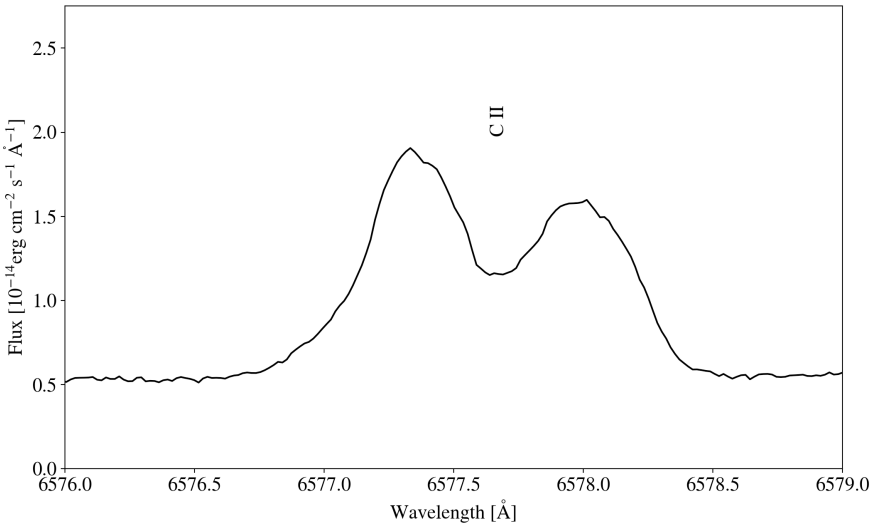

Figure 6. Spectrum region of NGC 3918 taken with the Ultraviolet-Visual Echelle Spectrograph (UVES), attached to the 8.2 m Kueyen (UT2) Very Large Telescope (VLT) (García-Rojas et al. 2015), where the C II λ6578 line is observed in detail. Due to the very high resolution of this spectrum (R$\sim \lambda/\Delta\lambda = 40,000$, which is equivalent to $\sim$ 6.5 km s^{-1}), it is possible to observe the expansion rate of the nebula, seeing the approaching and receding gas components (blueshift and redshift).

4 RESULTS AND DISCUSSION

In this chapter we show the results obtained following the methodology described in the previous chapter. The figures throughout this chapter show the results obtained for the set of Galactic PNe and H II regions included in DESIRED, highlighting the PNe behavior in some of the plots.

4.1 Recombination lines

Firstly, we study the behavior of the C II lines which excitation is, in principle, expected to be dominated by recombination: C II λ5342, λ6151, λ6462 and λ9903 with respect to the degree of ionization. To study the behavior of these lines we use their intensity ratios with respect to C II λ4267 line which is the most widely studied C II line in the optical spectrum. The permitted C II lines, in order to be RLs, have to originate from the capture of free electrons by the C^{++}, i.e., from C^{++} to C^{+}. This means that the intensity of the RLs will be proportional to the abundance of C^{++} and should be independent of the degree of ionization of the nebulae.

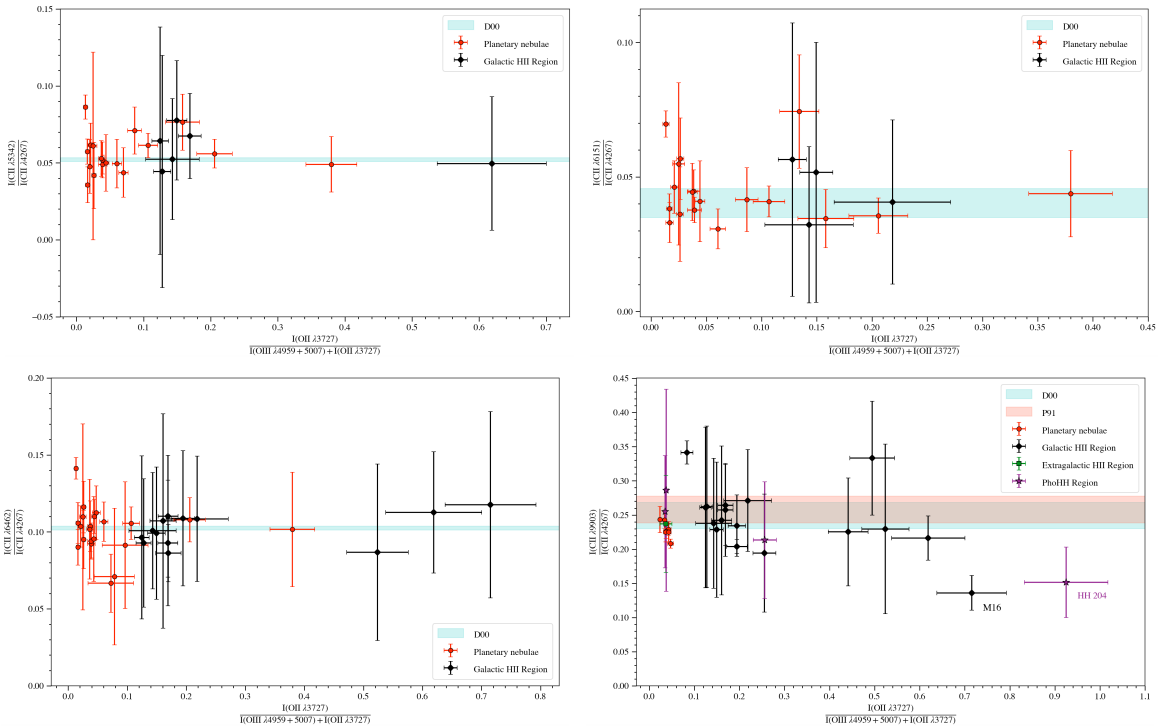

Figure 7. I (C II λ5342)/I (C II λ4267) (top left), I (C II λ6151)/I (C II λ4267) (top right), I (C II λ6462)/ /I (C II λ4267) (bottom left) and I (C II λ9903)/I (C II λ4267) (bottom right) ratios of all analyzed regions (Galactic PNe, Galactic H II regions, extragalactic H II regions and photoionized Herbig-Haro objects) with respect to the degree of ionization. The red band shows the theoretical ratio expected for nebular conditions between 4,000−15,000 K and 10^3 cm^{-3} according to the atomic data of Péquignot et al. (1991) (P91); the blue band shows the theoretical ratio expected adopting the atomic data of Davey et al. (2000) (D00). Notice that Péquignot et al. (1991) computations were only made for C II $\lambda\lambda$4267 and 9903 RLs.

In Figure 7 we plot the line ratios C II λ5342/C II λ4267, C II λ6151/C II λ4267, C IIλ6462/C II λ4267 and C II λ9903/C II λ4267 with respect to the degree of ionization (Equation 1) of the regions analyzed in this project. In addition, we also indicate the theoretical ratio expected considering typical nebular conditions between 4,000−15,000 K and 10^3 cm^{-3} according to the atomic data of Péquignot et al. (1991) and Davey et al. (2000) (red and blue bands respectively). We must bear in mind that Péquignot et al. (1991) computations were only made for C II $\lambda\lambda$4267 and 9903 RLs (see Table 3), whereas Davey et al. (2000) computations were made for all the lines considered.

A simple glance to these plots reveals that most of the data follow theoretical predictions, within observational uncertainties, assuming that both lines are excited by recombination. The few outliers

could be explained by different effects not taken into account in the original observations, such as telluric absorptions, blends with unidentified lines (there is a [Kr III] emission line close to C II λ9903 line that can be affecting some PNe data, or a complex velocity structure as is the case of HH 204 where it was difficult to deblend three different kinematic components (see Méndez-Delgado et al. 2021b). Therefore, we conclude that the C II permitted lines shown in Figure 7 (C II λ4267, C II λ5342, λ6151, λ6462, λ9903) are suitable indicators of the C^{++} abundances in PNe and H II regions.

4.2 C II λ3918+20

As we have pointed out in Chapter 3, the study of the excitation mechanism of the C II λ3918, λ3920 lines is very important as these transitions populate the upper level of the line analyzed in this project, C II λ6578 and, hence, their dominant excitation mechanism would have effects on the observed intensity of the C II λ6578 line.

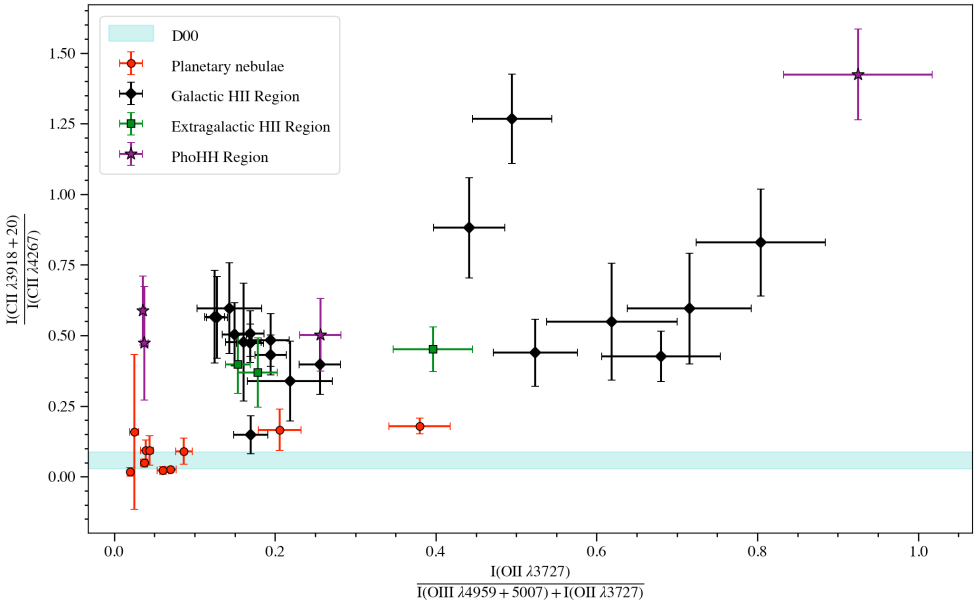

Figure 8. I (C II λ3918 + 20)/I (C II λ4267) ratio of all analyzed regions (Galactic PNe, Galactic H II regions, extragalactic H II regions and photoionized Herbig-Haro objects) with respect to the degree of ionization. The blue band shows the theoretical ratio expected for nebular conditions between 4,000−15,000 K and 10^3 cm^{-3} according to the atomic data of Davey et al. (2000) (D00). Notice that Péquignot et al. (1991) computations were not made for C II $\lambda\lambda$3918, 3920.

To verify which is the dominant mechanism in C II $\lambda\lambda$3918, 3920 lines, we represent the I(C II $\lambda\lambda$ 3918, 3920)/I(C II λ 4267) ratio with respect to the degree of ionization in Figure 8. We also plot the theoretical ratio expected considering typical nebular conditions between 4,000−15,000 K and 10^3 cm^{-3} according to the atomic data of Davey et al. (2000). Unfortunately, Péquignot et al. (1991) computations were not made for C II $\lambda\lambda$3918, 3920 lines.

Contrary to the C II line ratios analyzed in section 4.1, Figure 8 does not show a constant trend with the degree of ionization, but an increasing trend as the degree of ionization decreases. Therefore, we can conclude that in these lines, recombination is not necessarily the dominating excitation mechanism, and fluorescence is strongly acting as an excitation mechanism in many objects. It is important to note that most PNe are within the theoretical recombination predictions band, so the dominance of fluorescence in the excitation of these lines depend on the object. In the case of the H II regions it seems that we can conclude that the fluorescence dominates in C II $\lambda\lambda$3918, 3920 lines, while the PNe need to be analyzed in more detail.

As we have seen, these lines can be generated by two main mechanisms: i) the absorption of 638 Å photons by the C^+ (fluorescence) or ii) by direct recombinations of the C^{++} at the 4s level of the ^{2}S configuration; the former being the dominant one according to the results obtained, at least in H II

regions or, equivalently in objects with low degree of ionization where the amount of C^+ dominates over C^{++} and ^2S configurations are susceptible to excitation by UV photons from the ground level.

Summarizing, Figure 8 shows that the dominating process of the C II $\lambda\lambda$3918, 3920 lines is fluorescence, i.e, the intensities of the C II $\lambda\lambda$3918, 3920 lines are mostly proportional to the absorption of UV photons (continuum pumping) by the C^+, but will also have some proportionality with the recombinations of the C^{++}. The exception are PNe with the highest degree of ionization for which the line ratio is apparently consistent with theoretical predictions for nebular conditions between 4,000−15,000 K and 10^3 cm^{-3}. In principle, the general behavior found is in agreement with the work of Grandi (1976), where it was also concluded that the dominant mechanism in these lines was starlight fluorescence for the Orion nebula. However this author also concludes that the same mechanism should be responsible for the excitation of these lines in two relatively high degree of ionization PNe: NGC 7027 and NGC 7662 (I([O II] 3727)/(I([O II] 3727)+I([O III] 4959+5007)) <0.02, for references of their degree of ionization see Zhang et al. (2004) and Hyung & Aller (1997) respectively). This apparently contradictory results somehow illustrate that the relative importance of fluorescence excitation should be taken with some caution.

4.3 C II λ7231+36+37

As we have done with the C II $\lambda\lambda$3918, 3920 lines, we will check which is the dominant mechanism giving rise to the C II $\lambda\lambda$7231, 7236, 7237 lines through inspection of the the I (C II $\lambda7231+36+37$)/ /I (C II λ4267) ratio *vs*. the degree of ionization.

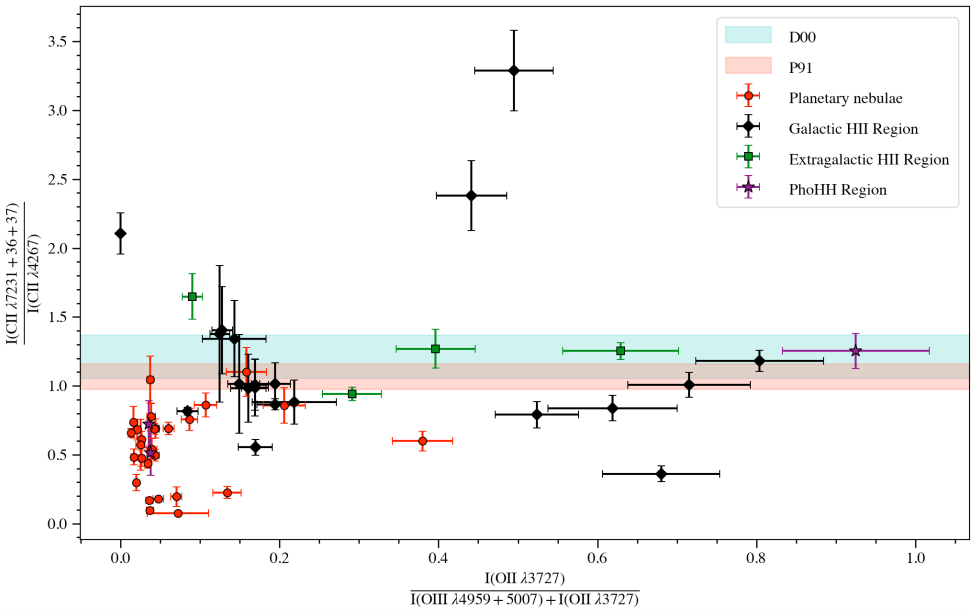

Figure 9. I (C II $\lambda\lambda7231+36+37$)/I (C II λ4267) ratio of all analyzed regions (Galactic PNe, Galactic H II regions, extragalactic H II regions and photoionized Herbig-Haro objects) with respect to the degree of ionization. The red band shows the theoretical ratio expected for nebular conditions between 4,000−15,000 K and 10^3 cm^{-3} according to the atomic data of Péquignot et al. (1991) (P91); the blue band shows the theoretical ratio expected adopting the atomic data of Davey et al. (2000) (D00).

In Figure 9 we show the I (C II $\lambda\lambda7231+36+37$)/I (C II λ4267) line ratio with respect to the degree of ionization along with the theoretical ratio expected for typical nebular conditions (4,000−15,000 K and 10^3 cm^{-3}) according to the atomic data of Péquignot et al. (1991) and Davey et al. (2000) (red and blue bands respectively). Contrary to the case of the C II $\lambda\lambda$3918, 3920 lines, this ratio do not show a clear dependence on the degree of ionization, and it seems that every case should be analyzed in a one-by-one basis.

As a general result, from the behavior shown in Figure 9, C II λ7231, λ7236 and λ7237 lines would have contributions from both starlight fluorescence and recombination, and the relative weight of each

mechanism would depend on the object. This result is in agreement with the conclusions raised by Grandi (1976) for the Orion nebula, who find that both mechanisms compete in the excitation of these transitions. We have to emphasize again that this line can be generated by three different mechanisms: i) absorption of 687 Å photons by C^+ (fluorescence), ii) direct recombination of C^{++} at the 3d level of the ^{2}D configuration and iii) cascade decays giving rise to the C II λ5889 and λ4267 lines (recombination). The ^{2}D level is susceptible to excitation by UV photons from the ground level. Therefore, the intensities of the C II λ7231, λ7236, λ7237 lines, which originates from this level, are not entirely proportional to the recombinations of the C^{++}, but also to the absorption of UV photons (continuum pumping) by the C^+, making it proportional to the abundance of C^+ when fluorescence dominates.

As we have done in the previous sections, if we compare the theoretical predictions according to the atomic data of Péquignot et al. (1991) and Davey et al. (2000) (red and blue bands respectively) with the observational data, it seems that in this case there is some kind of inconsistencies. As we have corroborated in section 4.1, the C II λ4267 line is excited by recombination so, in the case that C II $\lambda\lambda$ 7231, 7236, 7237 would be excited by an additional mechanism to recombination, observed line ratios should be above theoretical predictions, never below, which is the case for a large number of objects. This indicates errors in the calculations of the recombination coefficients for the C II $\lambda\lambda$ 7231, 7236, 7237 lines. It is not the scope of this work to evaluate recombination coefficients, however, what is clear is that in this case, even if recombination dominates the excitation of the lines, they cannot be used to compute C^{++} abundances.

4.4 C II λ6578

Finally, we focus on analyzing the behavior of the ratios of the C II λ6578 line with: (i) the C II λ4267 RL (Figures 10 and 11) for an analysis similar to the previous one in case this line is shown to be mainly excited by recombination as claimed by some authors; (ii) the C II λ3918, λ3920 lines (Figures 12 and 13), in whose generation fluorescence caused by absorption of 638 Å photons by C^+ dominates; (iii) the C II λ7231, λ7236, λ7237 lines (Figure 15), in which the fluorescence caused by the absorption of 687 Å photons by C^+ seem to be competing with direct recombinations, with a different weight of both processes depending on the object.

(i) I(C II λ6578)/I(C II λ4267) ratio:

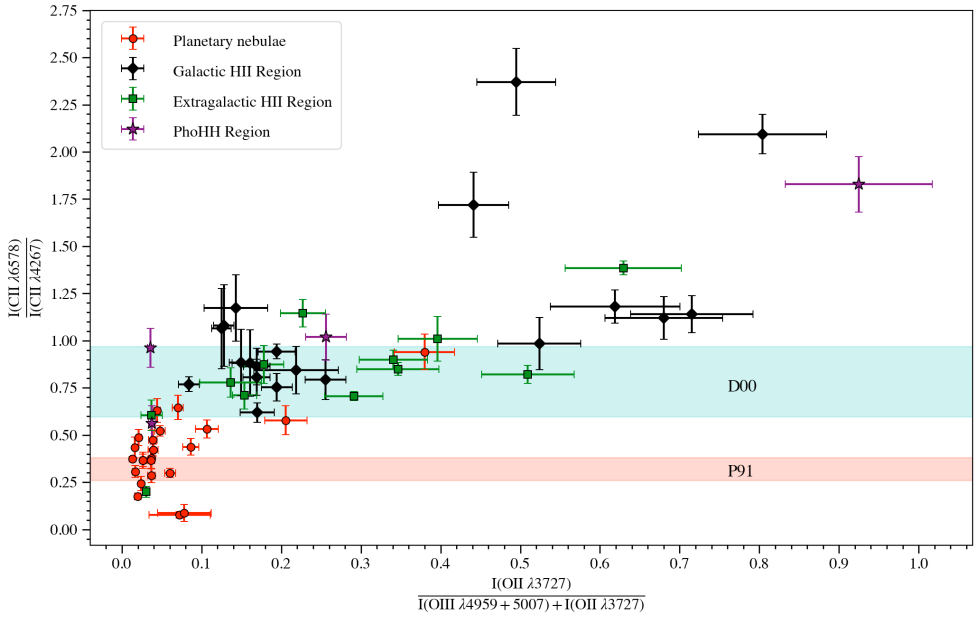

Figure 10. I (C II λ6578)/I (C II λ4267) ratio of all analyzed regions (Galactic PNe, Galactic H II regions, extragalactic H II regions and photoionized Herbig-Haro objects) with respect to the degree of ionization. The red band shows the theoretical ratio expected for nebular conditions between 4,000−15,000 K and 10^3 cm^{-3} according to the atomic data of Péquignot et al. (1991) (P91); the blue band shows the theoretical ratio expected adopting the atomic data of Davey et al. (2000) (D00).

Figure 10 shows the I(C II λ6578)/I(C II λ4267) ratio for all DESIRED nebulae having both lines measured with respect to the degree of ionization. And as in all the figures that we have seen so far, we have included the theoretical ratio expected for typical nebular conditions (4,000−15,000 K and 10^3 cm^{-3}) according to the atomic data of Péquignot et al. (1991) and Davey et al. (2000) (red and blue bands respectively).

The I(C II λ6578)/I(C II λ4267) line ratio shows a behavior similar to the I(C II $\lambda\lambda$3918 + 20)/ /I(C II λ4267) ratio, i.e., the ratio clearly increase with decreasing degree of ionization. Therefore, recombination is not the dominant mechanism in exciting this line and therefore, this line cannot be considered instead of C II λ4267 to compute reliable C^{++} abundances.

So, having ruled out direct recombination, we are left with two possible channels that populate the upper level of the C II λ6578 line (^{2}P^o) and both are fluorescence-related: i) cascade decays of the transitions giving rise to the C II λ7231, λ7236, λ7237 or ii) cascade decays of the transitions giving rise to the C II λ3918, λ3920 lines. Therefore, based on the results obtained, we can conclude that the dominant excitation mechanism of the C II λ6578 line is fluorescence. Furthermore, in the following we will see if both channels dominate equally or if there is one that dominates over the other.

Another result we obtain concerns the atomic data of Péquignot et al. (1991) and Davey et al. (2000) for this line. It is clear that atomic data of Davey et al. (2000) for the C II λ6578 line are not correct (the atomic data for C II λ4267 line have already been found to be correct as theoretical predictions are consistent with observed data as shown in Figure 7, in which the recombination line ratios were found to be very consistent with predictions of Davey et al. (2000)). This is manifested in the fact that the intensity ratios for most PNe are lower than theoretically predicted, which is known to be untrue, since the electronic temperatures of these nebulae fit within the color band considered (4,000−15,000 K). In contrast, the atomic data for Péquignot et al. (1991) appear to be adequate.

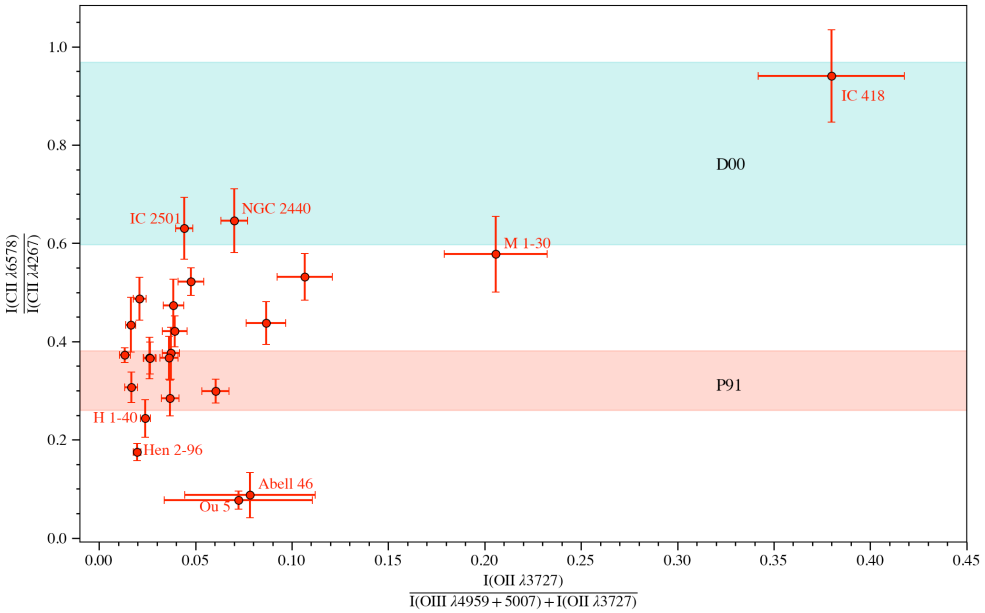

Figure 11. I (C II λ6578)/I (C II λ4267) ratio of PNe with respect to the degree of ionization. The red band shows the theoretical ratio expected for nebular conditions between 4,000−15,000 K and 10^3 cm^{-3} according to the atomic data of Péquignot et al. (1991) (P91); the blue band shows the theoretical ratio expected adopting the atomic data of Davey et al. (2000) (D00).

In Figure 11 we show an excerpt of Figure 10, focusing on PNe data. In this figure, it is clear that with the exception of few PNe, most of the objects are below the theoretical predictions by Davey et al. (2000). However, some of them are inside the band predicted by Péquignot et al. (1991), indicating that the latter seem to be in better agreement with the observed data. The two PNe with the lowest values of the line ratio: PN Ou5 and PN Abell 46, have large abundance discrepancies and therefore they are known to have a very low temperature gas component ($T_e \sim 10^3$ K) from which the recombination

line emission arises (Corradi et al. 2015, García-Rojas et al. 2022). The Péquignot et al. (1991) band depicted in the Figure 11 does not include these low temperatures.

Therefore, from these plots we can reach two main conclusions: i) the dominant mechanism of C II λ6578 line is not recombination, but continuum fluorescence in most of the cases; ii) the theoretical predictions for this line by Davey et al. (2000) for typical nebular conditions seem not being adequate, whereas the atomic data by Péquignot et al. (1991) seem to be much more consistent with what expected from the observations and therefore, should be used for chemical abundances computations.

(ii) I(C II λ6578)/I(C II λ3918 + 20) ratio:

Since it has already been proven that the mechanism that dominates the excitation of the C II λ6578 line is not recombination, but fluorescence, we aim to check which channel is the dominant to populate the upper level of this transition. We start with the first cascade decay of the transition that gives rise to the C II λ3918, λ3920 lines and populates the upper level of the C II λ6578 line. For this analysis, we evaluate the I(C II λ6578)/I(C II λ3918 + 20) line ratio vs. the degree of ionization, as shown in Figure 12.

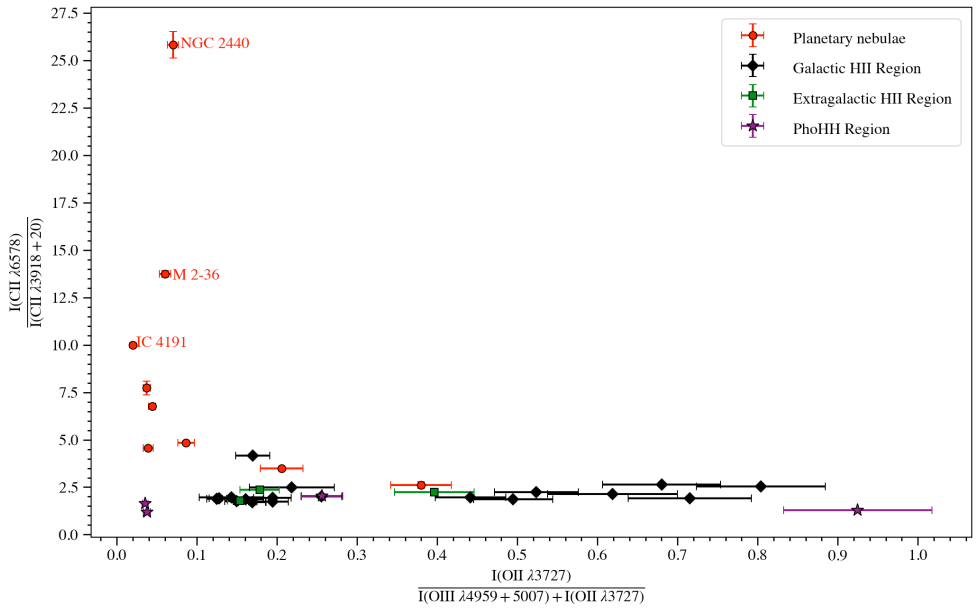

Figure 12. I (C II λ6578)/I (C II λ3918 + 20) ratio of all analyzed regions (Galactic PNe, Galactic H II regions, extragalactic H II regions and photoionized Herbig-Haro objects) with respect to the degree of ionization.

Figure 12 shows that the I(C II λ6578)/I(C II λ3918 + 20) ratio show a relatively constant value (around 1.90±0.09, Figure 13 shows in more detail) for most of the objects. Since C II λ3918, λ3920 are mostly populated by fluorescent excitation, this figure shows that C II λ6578 emission comes mainly from cascade decays of the transition giving rise to the C II $\lambda\lambda$3918, 3920 lines for most ionized regions, except for some PNe. For a small sample of highly excited PNe we obtain very large values of the I(C II λ6578)/I(C II λ3918 + 20) line ratio, which prevent us from being conclusive on this issue in these objects. As the I(C II λ6578)/I(C II λ3918 + 20) ratio remains practically constant at around 1.90±0.09 where the ratio takes values bellow 5, in Figure 13 we focus on this region of the plot. In tis figure we see more clearly this proportionality between both intensities for the H II regions. For PNe, besides the fact that the sample in which the C II λ3918, λ3920 lines were measured is small, there is a large dispersion in the data with values reaching ratio values greater than 10.

Furthermore, having obtained the mean value of the ratio (1.90±0.09), this would indicate that the absorption of 638 Å photons by the C^+ (fluorescence) that generates the C II $\lambda\lambda$3918, 3920 lines is almost twice that generates the C II λ6578 line.

It should be noted that in this sample there is a smaller number of data, since the C II λ3918, λ3920 lines are in the bluest region of the optical spectrum and has a rather faint intensity, being difficult to measure in some of the spectra of the database. These wavelengths are at the extreme end of the atmospheric window of the optical; for shorter wavelengths, the upper atmosphere completely blocks the radiation caused the ozone and ordinary oxygen. However, one of the checks that can be carried out is to subtract the intensity of the C II λ3918, λ3920 lines from the C II λ6578 line to see how much the fluorescence is affected by this channel (Figure 14) for the H II regions and PNe in which spectra the C II λ3918, λ3920 lines have been measured, through the ratio of intensities I (C II $\lambda 6578 - \lambda 3918 + 20$)/I (C II λ4267) and comparing with what we obtained in Figure 10.

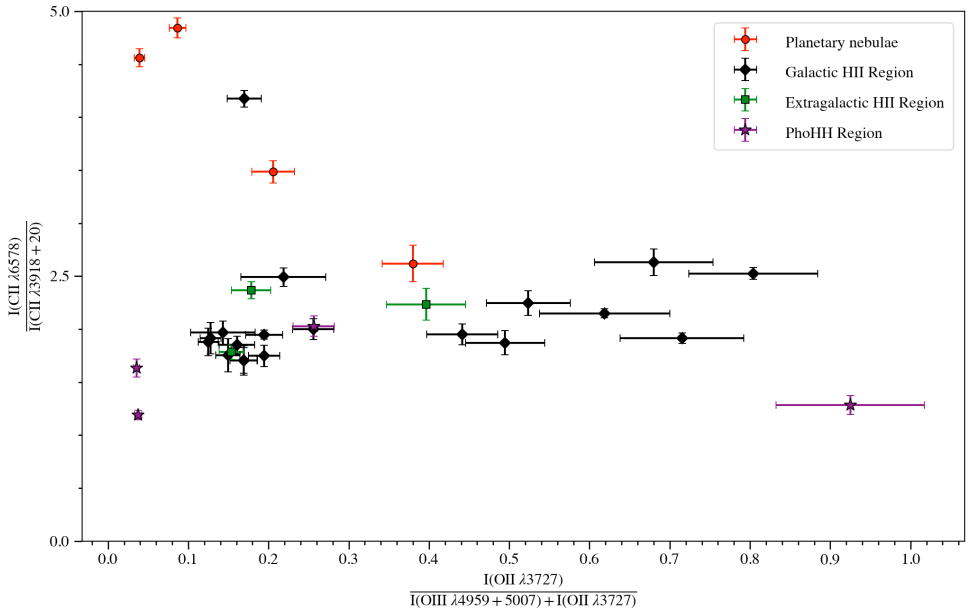

Figure 13. I (C II λ6578)/I (C II $\lambda 3918 + 20$) ratio of all analyzed regions (Galactic PNe, Galactic H II regions, extragalactic H II regions and photoionized Herbig-Haro objects) with respect to the degree of ionization. This plot is limited at 5.0 to observe the behavior of the lines ratio.

Therefore, from Figure 12 and Figure 13 we can say, in a general way, that for the C II λ6578 line of the spectra of the H II regions the main pumping channel is that of the C II $\lambda\lambda$3918, 3920 lines. For PNe this cannot be concluded, so we must see how it affects the other fluorescence channel, the one interconnecting this line with C II λ7231, λ7236, λ7237 lines. But before we get into this point, let's see what happens when we subtract the influence of the fluorescence of C II $\lambda\lambda$3918, 3920 lines to the C II λ6578 line, i.e, I(C $\lambda 6578 - \lambda 3918 + 20$).

Figure 14 shows the I (C II $\lambda 6578 - \lambda 3918 + 20$)/I (C II λ4267) ratio respect the degree of ionization for those regions in which the spectral lines considered for this intensity ratio have been measured. In addition, we have included the theoretical ratio expected for the same nebular conditions as in the previous cases.

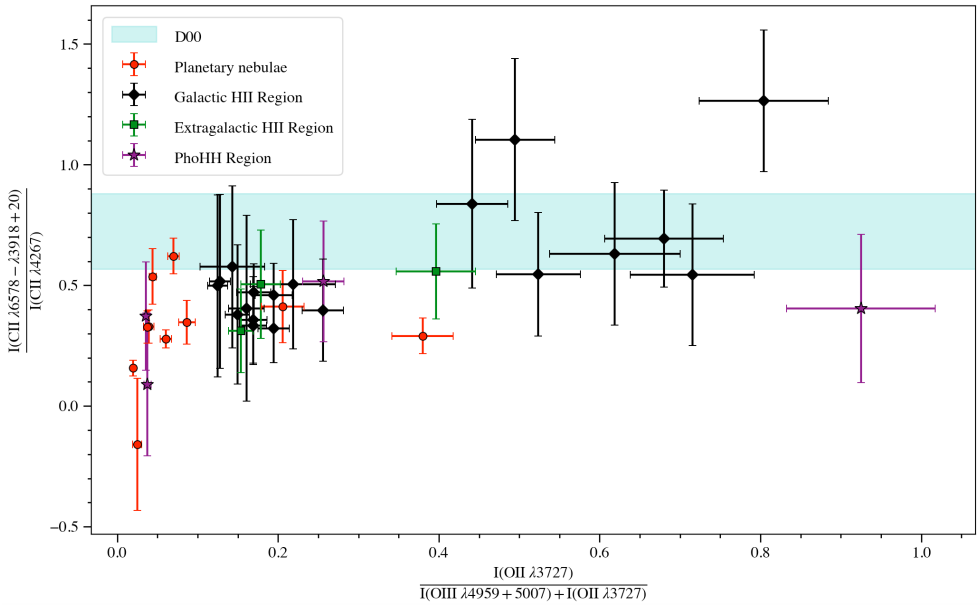

Figure 14. I (C II λ6578 − λ3918 + 20)/I (C II λ4267) ratio of all analyzed regions (Galactic PNe, Galactic H II regions, extragalactic H II regions and photoionized Herbig-Haro objects) with respect to the degree of ionization. The blue band shows the theoretical ratio expected for nebular conditions between 4,000−15,000 K and 10^3 cm^{-3} according to the atomic data of Davey et al. (2000) (D00). Notice that Péquignot et al. (1991) computations were not made for C II λ3920.

In this figure (Figure 14) it can be seen how for certain regions (mostly Galactic H II regions due to the number of data available for the rest of the regions) the fluorescence contribution of the channel that populates the lower level of the C II $\lambda\lambda$3918, 3920 lines seems to have been eliminated, indicating that for these regions this channel is the main one. The ratio follows the theoretical predictions (taking into account data uncertainties), although we had already seen that the theoretical predictions according to the atomic data of Davey et al. (2000) had errors in the computations (see Figure 10).

Therefore, for H II regions, we have shown that the main pumping channel populating the upper level of C II λ6578 line is that of the transition originating C II $\lambda\lambda$3918, 3920 lines. While the result for the PNe is not so clear, although in Figure 14, all except two PNe also follow the general trend.

(iii) I(C II λ6578)/I(C II λ7231 + 36 + 37) ratio:

The other mechanism for populating the upper level of the C II λ6578 line is the cascade decay of the transition that gives rise to the C II λ7231, λ7236, λ7237 lines, in which the fluorescence compete with recombination to be the main excitation mechanism (and that has been estimated to be of the order of 50% for each mechanism in the Orion nebula by Grandi 1976). Therefore, similarly to what is has been done before, we will make an inspection of the I(C II λ6578)/I(C II λ7231 + 36 + 37) line ratio with the degree of ionization. In Figure 15 we show this intensity ratio with respect to the degree of ionization and the theoretical predictions according to the atomic data of Davey et al. (2000) and Péquignot et al. (1991) (blue and red bands respectively).

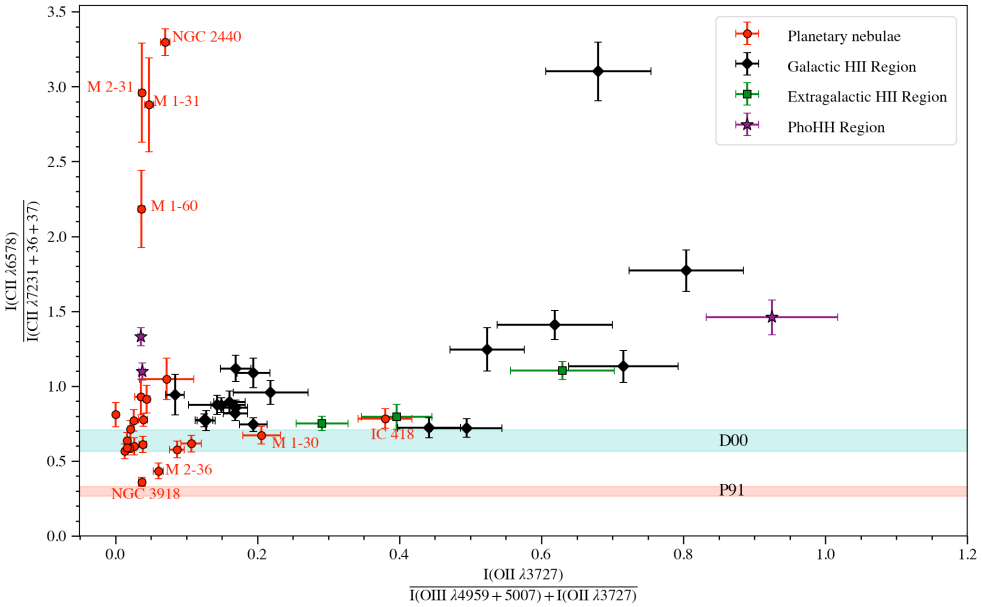

Figure 15. I (C II λ6578)/I (C II λ7231 + 36 + 37) ratio of all analyzed regions (Galactic PNe, Galactic H II regions, extragalactic H II regions and photoionized Herbig-Haro objects) with respect to the degree of ionization. The red band shows the theoretical ratio expected for nebular conditions between 4,000−15,000 K and 10^3 cm^{-3} according to the atomic data of Péquignot et al. (1991) (P91); the blue band shows the theoretical ratio expected adopting the atomic data of Davey et al. (2000) (D00).

In this figure we see how there seems to be some dependence with the degree of ionization, which may be an indication that the main fluorescence channel is that of the C II $\lambda\lambda$3918, 3920 lines. However, if we focus on the PNe, excluding those with very large values of the ratio, they are more or less concentrated around a constant value. We have already found that the theoretical predictions adopting the atomic data of Davey et al. (2000) and the atomic data of Péquignot et al. (1991) present discrepancies with observational results in the case of the C II $\lambda\lambda$7231, 7236, 7237 lines (see Section 4.3). In addition, in Section 4.4 we concluded that the computations by Davey et al. (2000) for the C II λ6578 transition are not adequate either. This implies that the consistency between the convergence of the PNe and the band predicted by Davey et al. (2000) may be coincidental.

Therefore, in general, the main channel of fluorescence of the C II λ6578 line is the one that populates the lower level of C II $\lambda\lambda$3918, 3920 lines (which is the upper level of C II λ6578 line). But in the case of PNe a more detailed analysis must be carried out. Depending on the object, the fluorescence would come more from one channel or another and the contribution of this would be greater or lesser. In some cases the major contribution of fluorescence would come from the channel of the C II $\lambda\lambda$7231, 7236, 7237 lines.

4.5 Discussion

After having analyzed which mechanism dominates the generation of C II λ6578 line by means of ratios of line intensities (λ4267, λ3918, λ3920 and λ7231, λ7236, λ7237), we will discuss the results obtained here and we will take into account the results published to date.

(i) Recombination lines

We have verified that C II λ5342, λ6151, λ6462 and λ9903 lines are pure RLs, in agreement with Escalante et al. (2012), where the intensity ratio due recombination of these lines through the ratio $I_{\rm rec}/I_{\rm calc}$ were 1.000, 0.969, 1.000 and - (not calculated), respectively (see Table 5 of the article).

We have to bear in mind, however, that Escalante et al. (2012) did the analysis for a particular object, the planetary nebula IC 418; whereas in our case we have done it in a general way for a set of 190 nebulae spectra.

(ii) C II λλ3918, 3920 and C II λ7231, λ7236, λ7237

In this project we have verified that the C II λ3918, λ3920 lines are generated mainly by fluorescence mechanisms and the C II λ7231, λ7236, λ7237 lines have a fluorescence component and a recombination component, in agreement with the results obtained by Grandi (1976) where the spectra of faint permitted lines of the Orion Nebula and the PNe NGC 7027 and NGC 7662 were analyzed. Grandi (1976) identified the dominant excitation mechanism of each of the observed lines (see Table 2 of the article where these two lines appear) and, with the exception of some lines, calculated models showing the different excitation mechanisms of these lines.

Regarding the results of Escalante et al. (2012), they are focused in a single object and we had seen that for the C II λ7231, λ7236, λ7237 lines, the dominating excitation mechanism depends on the object (a well-defined general behavior is not observed). Their intensity ratios due recombination of these lines were 0.632, 0.836 and 0.632 respectively, i.e., the main contribution is recombination, but we cannot forget the contribution of fluorescence (∼37 % for λ7231, λ7237 lines and ∼16 % for λ7236 line).
On the contrary, and in agreement with our general result, they obtained that the main contribution to the excitation of C II λλ3918, 3920 lines is fluorescence (by ∼90%).

Thus, in this work we have verified using a different methodology than in previous works, that the dominant excitation mechanism in the transition that originates the C II λ7231, λ7236, λ7237 lines depends on the object, with the percentages of fluorescence and recombination contributions varying from one to another. On the other hand, we have also confirmed that for the C II λλ3918, 3920 lines, the main contribution to their excitation is fluorescence.

(iii) C II λ6578

In this project we have obtained that the C II λ6578 line is dominated by fluorescence, contrary to the work of Escalante et al. (2012), where they obtained that the C II λ6578 line is dominated by recombination. The authors compared calculated intensities of lines of C II and other elements with a published deep spectroscopic of the planetary nebula IC 418 and they calculated the intensity fraction due to recombination, $I_{\rm rec}/I_{\rm calc}$, this value being 0.654 (Table 5 of the article). However, we have to take into account that Escalante et al. (2012) did the work for a particular object and in fact, their conclusion is that the fluorescence contribution is quite important (about 35 %). In our study, for the degree of ionization of IC 418, the contribution we estimate is much higher than the one calculated in that work (see Figure 11).

In the work of Richer et al. (2017) they presented spectroscopic observations of the C II λ6578 permitted line for 83 lines of sight in 76 PNe at high spectral resolution. The authors studied the kinematics of the C II λ6578 permitted line with respect to other permitted lines and CELs. And statistically, they found that the kinematics of C II λ6578 line are not those expected if this line arises from the recombination of C^{++} ions or the fluorescence of C^{+} ions in ionization equilibrium in a chemically homogeneous

nebular plasma, but instead its kinematics are those appropriate for a volume more internal than expected. However, our results point to a much important influence of the fluorescence in the intensity of this line than that adopted in Richer et al. (2017) which was estimated through a grid of photoionization models adopting different ionization sources described as blackbodies. Therefore, our results put the conclusions of this work on hold, as fluorescence contribution seem to completely dominate the emission of C II λ6578 line for H II regions and PNe with intermediate to low excitations.

(iv) Atomic data of Davey et al. (2000) and Péquignot et al. (1991)

Throughout the analysis of the excitation mechanisms of the C II λ6578 line, we have used the atomic data of Davey et al. (2000) and Péquignot et al. (1991), where it has been observed that the data of Davey et al. (2000) are not correct for this line. In addition, it appears that these authors made a proportional error in the calculations for the C II λ7236 line, since if we look at Figure 15 it would appear that the atomic data for both lines are correct. On the contrary, it seems that the atomic data of Péquignot et al. (1991) for the C II λ6578 line agree much better with the observational results presented in this work.

Therefore, it would be necessary to review atomic data computations by Davey et al. (2000) at least for C II λ6578 and C II $\lambda\lambda$7231, 7236, 7237 lines, as the theoretical ratio expected for nebular conditions between 4,000−15,000 K and 10^3 cm^{-3} according to these atomic data does not correspond to the results obtained from observed spectra.

5 CONCLUSIONS

In this project we have analyzed which excitation mechanism dominates the transition that gives rise to the C II λ6578 permitted line as well as different C II transitions. We use DESIRED, a database of 190 deep optical spectra of photoionized nebulae (72 of them correspond to extragalactic H II regions, 56 to Galactic H II regions, 34 to Galactic PNe, 21 to Galactic ring nebulae around massive stars, 6 to photoionized Herbig-Haro objects and 1 proplyd, the last two sets corresponding to objects immersed in the Orion Nebula).

Our motivation to focus on C II λ6578 is that is easily observable in multitude of objects and is very close to Hα. The latter means that the possible errors in the flux calibration or in the extinction correction are minimized, in contrast to other permitted lines such as C II λ4267. A good understanding of the excitation mechanisms of C II λ6578 can be important to address the abundance discrepancy (AD) problem.

We also verify the main excitation mechanisms of the following C II lines: $\lambda\lambda$3918, 3920, 7231, 7236, 7237, 4267, 5243, 6151, 6462 and 9903. In Table 4 we show our main results, indicating the excitation mechanisms of the C II lines as well as the atomic configuration and the atomic level (we do not specify fine structure configuration).

Our methodology is very simple and direct as we have not gone object by object evaluating the influence of fluorescence using detailed SED and object models.

Laboratory wavelength [Å]	Spc	Configuration	Term	Dominant Mechanism
4267.001	C II	$2s^2.3d$-$2s^2.4f$	^2D-$^2F^o$	Recombination
5342.500	C II	$2s^2.4f$-$2s^2.7g$	$^2F^o$-^2G	Recombination
6151.530	C II	$2s^2.4d$-$2s^2.6f$	^2D-$^2F^o$	Recombination
6461.950	C II	$2s^2.4f$-$2s^2.6g$	$^2F^o$-^2G	Recombination
9903.890	C II	$2s^2.4f$-$2s^2.5g$	$^2F^o$-^2G	Recombination
3918.978	C II	$2s^2.3p$-$2s^2.4s$	$^2P^o$-^2S	Fluorescence
3920.693	C II	$2s^2.3p$-$2s^2.4s$	$^2P^o$-^2S	Fluorescence
6578.048	C II	$2s^2.3s$-$2s^2.3p$	^2S-$^2P^o$	Fluorescence
7231.340	C II	$2s^2.3p$-$2s^2.3d$	$^2P^o$-^2D	Fluorescence/Recombination
7236.420	C II	$2s^2.3p$-$2s^2.3d$	$^2P^o$-^2D	Fluorescence/Recombination
7237.170	C II	$2s^2.3p$-$2s^2.3d$	$^2P^o$-^2D	Fluorescence/Recombination

Table 4. Electronic configurations and dominant mechanism of the different transitions that originate the C II lines of this project.

The results of this work shows that the C II λ5342, λ6151, λ6462 and λ9903 are RLs, as C II λ4267. This is consistent with the conclusions of Escalante et al. (2012) based on the single planetary nebula IC 418.

Our work conclude that C II $\lambda\lambda$3918, 3920 lines are excited mainly by fluorescence whereas C II $\lambda\lambda$7231, 7236, 7237 have both contributions from fluorescence and a recombinations. This results are in agreement with the studies of Grandi 1976 and Escalante et al. (2012) based on few objects.

Finally, we demonstrate that the dominant mechanism of C II is continuum fluorescence in most cases. From our simple approach, we qualitatively estimate that the contribution of the fluorescence is higher than the one estimated by Richer et al. (2017), which was based on a grid of photoionization models adopting different ionization sources described as blackbodies.

Our conclusions are not intended to be quantitative models of the fraction of fluorescence contained in the studied lines for all objects, but rather to determine whether or not this mechanism dominates the line excitation. A quantitative determination of this type requires a complete understanding of the main

and secondary mechanisms that give rise to fluorescence, which, as mentioned, is very complex.

Since the dominant mechanism for the C II λ6578 line is fluorescence, this cannot be considered for works related to the AD problem. The major problem facing the study of AD is the intrinsic faintness of heavy element RLs, generally three to four orders of magnitude fainter than the intensity of Hβ, which necessitates the use of high sensitivity spectrographs and large aperture telescopes. An additional problem is that recombination may not be the main excitation mechanism of these lines, as has been demonstrated to be the case for the C II λ6578 line. Moreover, we have been able to demonstrate which is the dominant excitation mechanism in the transition that gives rise to this line in a relatively simple and generalized way instead of studying each object individually, which is the canonical way but also much more complicated and time-demanding, given the close relationship between continuum fluorescense with the spectral energy distribution (SED) of the ionizing source.

In addition, due to the need of comparing with theoretical predictions, we have concluded that a revision of the atomic data for the C II λ6578 and $\lambda\lambda$7231, 7236, 7237 lines from the work of Davey et al. (2000) is required. And that the atomic data of Péquignot et al. (1991), although older than Davey et al. (2000), are more in line with the observations.

As future work, a similar methodology could be carried out for other relatively well observed permitted lines in the optical spectra, such as the N II lines, since something similar occurs with these lines. Moreover, with the continuous improvement of spectroscopic techniques and the increase in the number of studies aimed at characterizing PNe and H II regions in our galaxy, it will be possible to obtain results from a larger sample with high-quality data. Future studies of data taken with the new multi-object spectrographs on 4-meter class telescopes such as WEAVE will eventually provide a more complete sample of nebulae.

6 REFERENCES

Aller L. H., 1984, *Physics of Thermal Gaseous Nebulae*, Springer Netherlands

Aller L. H., Baker J. G. & Menzel, D. H., 1939, ApJ, 89, 587

Baker J. G. & Menzel D. H., 1938, ApJ, 88, 52

Corradi R. L. M., García-Rojas J., Jones D., Rodríguez-Gil P., 2015, ApJ, 803, 99

Davey A. R., Storey P. J., Kisielius R., 2000, A&AS, 142, 85

Escalante V., 1989, In Proceedings of the 131st symposium of the IAU Torres-Peimbert S. (eds) Planetary Nebulae, vol 131, Springer, Dordrecht

Escalante V., Morisset C., Georgiev L., 2012, MNRAS, 426, 2318

Esteban C., Peimbert M., Torres-Peimbert S., Escalante V. 1998, MNRAS, 295, 401

Ferland G. J., Henney W. J., O'Dell C. R., Porter R. L., van Hoof P. A. M., Williams R. J. R., 2012, ApJ, 757, Issue 1, article id. 79, 18

Ferland G. J., Henney W. J.,O'Dell C. R., Peimbert M., 2016, RevMexAA, 52, 261

Frankowski A. & Soker N., 2009, New Astronomy, 14, 654

Frew D. J., Bojičić I. S., Parker Q. A., 2013, MNRAS, 431, 2

García-Rojas J., Madonna S., Luridiana V., Sterling N. C., Morisset C., Delgado-Inglada G., Toribio San Cipriano L., 2015, MNRAS, 452, 2606

García-Rojas J., Wesson R., Boffin H. M.J., Jones D., Corradi R. L. M., Esteban C., Rodríguez-Gil P., 2019, arXiv e-prints, p. arXiv:1904.06763

García-Rojas J., 2020, *Physical Conditions and Chemical Abundances in Photoionized Nebulae from Optical Spectra.* In: Kabáth P., Jones D., Skarka M. (eds), *Reviews in Frontiers of Modern Astrophysics*, Springer

García-Rojas J., Morisset C., Jones D.,Wesson R., Boffin H. M. J., Monteiro H., Corradi R. L. M., Rodríguez-Gil P., 2022, MNRAS, 510, 5444

Grandi S. A., 1975a, ApJ, 196, 465

Grandi S. A., 1975b, ApJ (Letters), 199, L43

Grandi S. A., 1976, ApJ, 206, 658

Hyung S. & Aller L. H., 1997, ApJ, 491, 242

Lucy L. B, A&A, 1995, 294, 555

Luridiana V., Morisset C., Shaw R. A., 2015, A&A, 573, A42
Maciel W. J., Costa R. D. D., Idiart T. E. P., 2009, RevMexAA, 45, 127

Méndez-Delgado J. E., Henney W. J., Esteban C., García-Rojas J., Mesa-Delgado A., Arellano-Córdova K. Z., 2021b, ApJ, 918, 27

Méndez-Delgado J. E., Esteban C., García-Rojas J., Arellano-Córdova K. Z., Kreckel K., Gómez-Llanos V., Egorov O., Peimbert M., Orte-García M., 2023, MNRAS, submitted

Mesa-Delgado A., Núñez-Díaz M., Esteban C., García-Rojas J., Flores-Fajardo N., López-Martín L., Tsamis Y. G., Henney W. J., 2012, MNRAS, 426, 614

Moore C.E. & Merrill P.W., *Partial Grotrian Diagrams of Astrophysical Interest*, NSRDS National Bureau of Standards, Vol. 23 (1968)

Osterbrock D. E. & Ferland G. J., *Astrophysics of Gaseous Nebulae and Active Galactic Nuclei*, University Science Books, Second Edition

Peimbert M., Peimbert A., Delgado-Inglada G., 2017, PASP, 129, 082001

Péquignot D., Petitjean P., Boisson C., 1991, A&A, 251, 680

Richer M. G., Súarez G., López J. A., García Díaz M. T., 2017, AJ, 153, 140

Rodríguez M., 1999, A&A, 348, 222

Ruiz-Escobedo F. & Peña M., 2022, MNRAS, 500, 5984

Seaton M. J., 1968, MNRAS, 139, 129

Zhang Y., Liu X. -W., Luo S. -G., Péquignot D., Barlow M. J., 2004, A&A, 442, 249

7 ACKNOWLEDGEMENTS

Probablemente esta sea la sección más cursi de la memoria, pero necesaria para concluir un trabajo como este y tras haber pasado seis años desde que me metí en este mundo de la Física y Astrofísica. Todavía me resulta difícil de creer que ya esté aquí y que hayan pasado todos estos años tan rápido y durante los cuales he conocido gente maravillosa, siendo los aquí mencionados los que más me han marcado y apoyado.

En primer lugar me gustaría agradecer a mis dos tutores, Jorge y Eduardo, por enseñarme todo lo tratado durante el transcurso del trabajo y haberme dejado empezar desde antes de verano de 2022. Por sus correcciones y respuestas bastante rápidas cuando tenía una duda. He aprendido muchísimo y me ha encantado mucho trabajar con ustedes, hasta tal punto que el siguiente paso que me gustaría dar es un doctorado en el grupo de Nebulosas.

Gracias a César por tu ayuda prestada, aún no siendo mi tutor oficial del trabajo, pero siéndolo para mí. Además por tus clases de Nebulosas en 1º de Máster, haciendome descubrir este mundillo de las Nebulosas y haberme dado la oportunidad de hacer el trabajo con tu grupo. Quién me iba a decir en 1º de carrera que al final haría el TFM con ustedes.

También me gustaría agradecer a Pablo, mi tutor de carrera, de TFG (y casi que de vida) y profesor tanto de Grado como de Máster. Gracias por animarme a seguir en esto desde el primer día, darme tus consejos y confianza. Espero seguir en contacto contigo, aunque me haya alejado un poco de las enanas blancas y binarias (solo un poco porque aquí sigo con ellas en las nebulosas planetarias). Gracias por estos seis años en los que has sido uno de mis ejemplos a seguir.

Gracias a mis amigos y compañeros del Máster: Alba, Aina, Iliana, Daniel y Samuel. Me llevo la bonita amistad que hemos hecho durante estos dos años bastante intensos. Gracias por aguantar mis bajones y trabadas de cabeza y saber sacarme de ellos. Especial mención a Iliana, la persona más amorosa que conozco, que aunque te vayas a tantos kilómetros de aquí, espero poder seguir manteniendo contacto (y algún día ir a México).

Gracias a Guillem por las liadas y desliadas de cabeza, por estar siempre ahí y tu apoyo mostrado estos dos últimos años. Te he cogido un cariño y aprecio especial que será difícil de perder. Te agradezco tu disposición siempre que necesitaba hablar con alguien un ratito y poder contarte cosas que no podía contar a los demás.

Y como no, no me voy a olvidar del astropiso: Pau, María y Yéssica; los tres son personas increíbles que no voy a olvidar y con los cuales espero seguir en contacto. Gracias por sus ánimos para seguir y espero que puedan conseguir todo lo que se propongan y que aunque se vayan lejos, nos veamos cuando vuelvan por Tenerife.

Por último, pero no menos importante, agradecer a mis amigos del Grado: Raúl, Sara, Susana y Nuria. Otra bonita amistad que me llevo de la universidad y a los cuales animo por el camino que les queda por recorrer, el cual es muy bonito y aunque cueste, la satisfacción de llegar al final y mirar hacia atrás todo lo que has hecho no tiene precio y verán que todo ha valido la pena.